NASA/CR-1998-207642

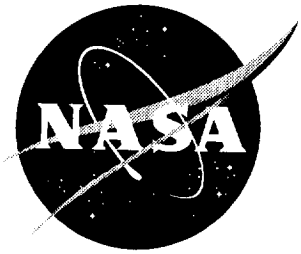

Fabrication and Testing of Mo-Re Heat Pipes Embedded in Carbon/Carbon

David E. Glass
Analytical Services & Materials, Inc., Hampton, VA

Michael A. Merrigan and J. Tom Sena
Los Alamos National Laboratory, Los Alamos, NM

National Aeronautics and
Space Administration

Langley Research Center
Hampton, Virginia 23681-2199

Prepared for Langley Research Center
under Contract NAS1-96014

March 1998

The use of trademarks or names of manufacturers in this report is for accurate reporting and does not constitute an official endorsement, either expressed or implied, of such products or manufacturers by the National Aeronautics and Space Adminstration or by Analytical Services & Materials, Inc.

Available from the following:

NASA Center for AeroSpace Information (CASI)
800 Elkridge Landing Road
Linthicum Heights, MD 21090-2934
(301) 621-0390

National Technical Information Service (NTIS)
5285 Port Royal Road
Springfield, VA 22161-2171
(703) 487-4650

Fabrication and Testing of Mo-Re Heat Pipes Embedded in Carbon/Carbon

David E. Glass
Analytical Services & Materials, Inc., Hampton, VA

Michael A. Merrigan and J. Tom Sena
Los Alamos National Laboratory, Los Alamos, NM

Abstract

Refractory-composite/heat-pipe-cooled wing and tail leading edges are being considered for use on hypersonic vehicles to limit maximum temperatures to values below material reuse limits and to eliminate the need to actively cool the leading edges. The development of a refractory-composite/heat-pipe-cooled leading edge has evolved from the design stage to the fabrication and testing of heat pipes embedded in carbon/carbon (C/C). A three-foot-long, molybdenum-rhenium heat pipe with a lithium working fluid was fabricated and tested at an operating temperature of 2460°F to verify the individual heat-pipe design. Following the fabrication of this heat pipe, three additional heat pipes were fabricated and embedded in C/C. The C/C heat-pipe test article was successfully tested using quartz lamps in a vacuum chamber in both a horizontal and vertical orientation. Start up and steady state data are presented for the C/C heat-pipe test article. Radiography and eddy current evaluations were performed on the test article.

Introduction

Stagnation regions, such as wing and tail leading edges and nose caps, are critical design areas for hypersonic aerospace vehicles because of the hostile thermal environment those regions experience during flight. As a hypersonic vehicle travels through the earth's atmosphere, the high local heating and aerodynamic forces cause extremely high temperatures, severe thermal gradients, and high stresses. Analytical studies and laboratory and wind tunnel tests [1-12] indicate that a solution to the thermal-structural problems associated with stagnation regions of hypersonic aerospace vehicles might be alleviated by the use of heat pipes to cool these regions. Recent work to develop a novel refractory-composite/refractory-metal heat-pipe-cooled leading-edge concept for hypersonic vehicles combines advanced high-temperature materials, coatings, and fabrication techniques with an innovative thermal-structural design. Preliminary design studies [13] indicate that a heat-pipe-cooled leading edge can reduce the leading-edge mass significantly compared to an actively cooled leading edge, can completely eliminate the need for active cooling, and has the potential to provide failsafe and redundant features.

The present paper discusses several tests to help verify the fabrication and performance of a heat-pipe-cooled leading edge for hypersonic vehicles. A three-foot-long molybdenum-rhenium (Mo-Re) "D-shaped" heat pipe was fabricated and heated with induction heating in a vacuum chamber to an operational temperature of 2460°F. The heat pipe used lithium as the working fluid and had a "D-shaped" cross-section. The heat-pipe wick was constructed of 400 x 400 mesh Mo-Re screen with a single artery along the length of the heat pipe. The same design was used to construct three additional heat pipes which were embedded in C/C. The C/C test article was then tested with quartz lamps in a vacuum chamber in both the vertical and horizontal orientation. All of the heat-pipe fabrication was performed at Los Alamos National Laboratory (LANL) and the testing was performed both at LANL and NASA Langley Research Center.

Description of Heat-Pipe-Cooled Leading-Edge Concept

Heat pipes are being considered for use on both the wing and vertical tails of hypersonic vehicles. A brief description of how heat pipes operate and are applied for leading-edge cooling is first presented, followed by a description of the proposed heat-pipe-cooled leading-edge concept.

Leading-Edge Heat-Pipe Operation

Heat pipes transfer heat nearly isothermally by the evaporation and condensation of a working fluid, as illustrated in Figure 1. The heat is absorbed within the heat pipe by evaporation of the working fluid. The evaporation results in an internal pressure differential that causes the vapor to flow from the evaporator region to the condenser region, where it condenses and gives up heat. The cycle is completed with the return flow of the liquid condensate to the evaporator region by the capillary action of a wick.

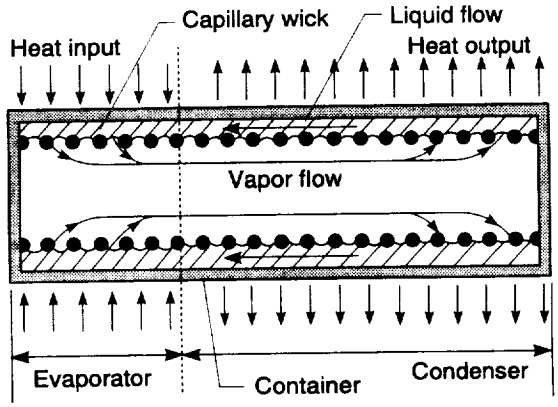

Figure 1: Schematic diagram of the operation of a heat pipe showing the heat-pipe container, working fluid, and wick.

Heat pipes provide cooling of the stagnation region by transferring heat nearly isothermally to locations aft of the stagnation region, thus raising the temperature aft of the stagnation region above the expected radiation equilibrium temperature. When applied to leading-edge cooling, heat pipes operate by accepting heat at a high rate over a small area near the stagnation region and radiating it at a lower rate over a larger surface area, as shown in Figure 2. The use of heat pipes results in a nearly isothermal leading-edge surface; reducing the temperatures in the stagnation region and raising the temperatures of both the upper and lower aft surfaces.

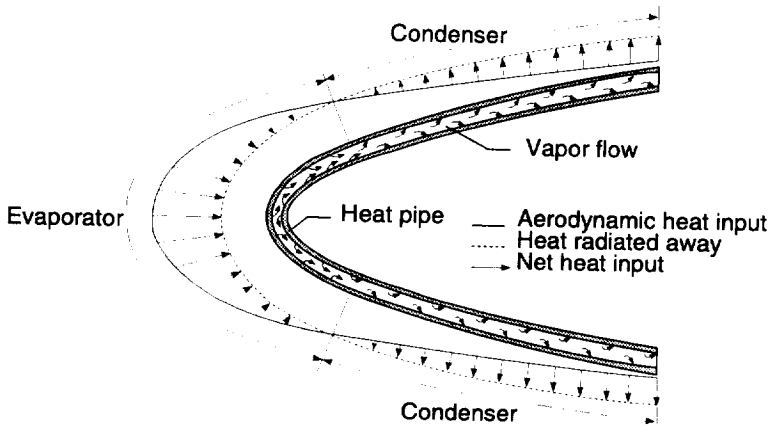

Figure 2: Schematic diagram of a heat-pipe-cooled leading edge showing regions of net heat input (evaporator) and net heat output (condenser).

Carbon/Carbon Heat-Pipe-Cooled Wing-Leading-Edge

A C/C heat-pipe-cooled wing-leading-edge is illustrated in Figure 3 [14]. The heat pipes are oriented normal to the leading edge and have a "D-shaped" cross section, with the flat part of the "D" forming the wing-leading-edge outer surface. A cross section of the leading edge is shown in Figure 3 illustrating the "D-shaped" heat pipes embedded in the C/C. An alternating J-tube configuration was selected to minimize heat-pipe spacing in the nose region where heating is highest, and at the same time minimize mass. The C/C structure sustains most of the mechanical structural loads and also offers ablative protection in the event of a heat-pipe failure.

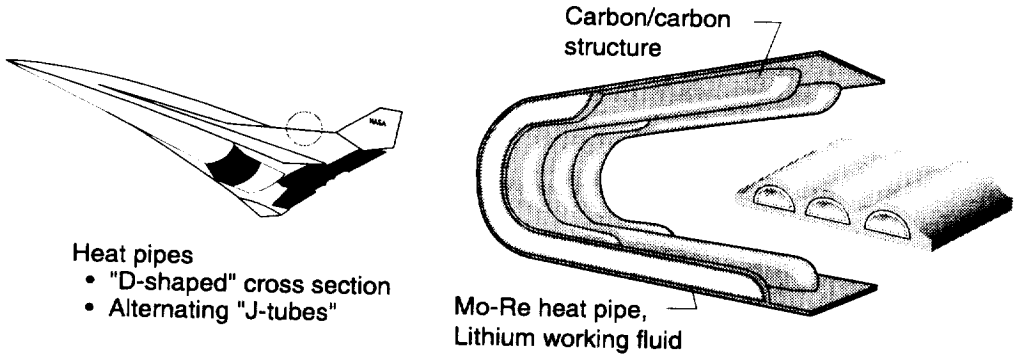

Figure 3: Schematic drawing of a hypersonic vehicle with a diagram of a heat-pipe-cooled wing leading edge.

The maximum operating temperature capability of coated C/C composite materials for the primary structure of the leading edge is high (~3000°F) relative to refractory metals, which are typically limited to approximately 2400°F. The potentially higher operating temperature of the present concept increases the radiation heat-rejection efficiency of the heat-pipe-cooled leading edge and permits reductions in the mass of the leading edge for a given leading-edge radius. In addition, the higher operating temperature increases the total heat load that can be accommodated passively by the heat pipe (i.e., no forced convective cooling required). For many trajectories, the high operating temperatures of the present design help eliminate the need for active cooling during both ascent and descent, thus eliminating the need for carrying additional hydrogen fuel (coolant) into orbit. Since many hypersonic vehicles return unpowered for

landing, the additional hydrogen fuel needed for cooling during descent would result in a mass penalty.

Results and Discussion

Initially, a single heat pipe with a "D-shaped" cross section was fabricated and tested to 2460°F in a vacuum. Upon determining that the heat-pipe design was adequate, three additional heat pipes were fabricated. These three heat pipes were then embedded in C/C and tested in a vacuum chamber. A discussion of each of these heat-pipe tests follows.

Design Validation Heat Pipe

A "D-shaped" heat pipe was fabricated and tested to determine the performance characteristics of the heat pipe designed for cooling the wing leading edge. A description of the fabrication procedure for the heat pipe is given followed by a discussion of the heat-pipe testing. Both the fabrication and testing of the design validation heat pipe were performed at LANL.

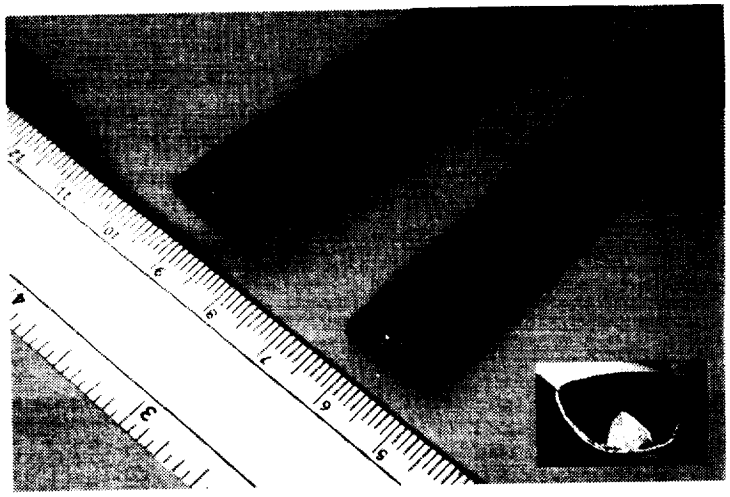

Figure 4: Photograph of a section of "D-tube" and screen wick.

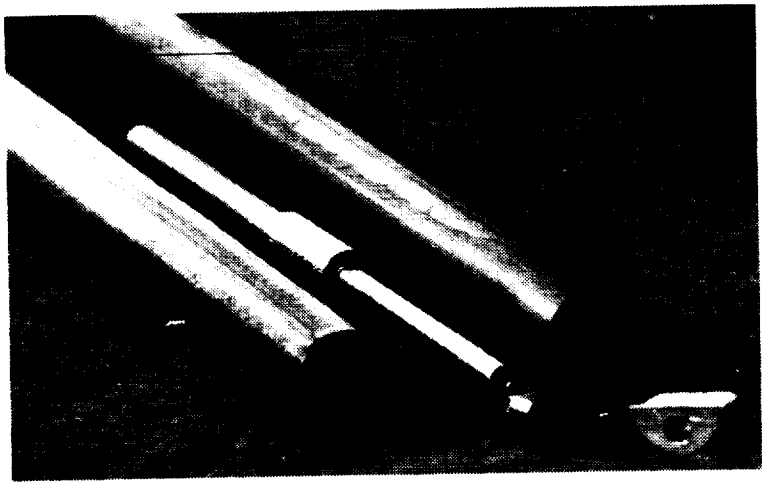

Figure 5 Photograph of the parts of the heat pipe prior to final welding, showing the "D-shaped" screen wick, heat-pipe container, end caps, and fill tube.

The heat pipe was fabricated from a Mo-41Re "D-shaped" tube that was drawn from an arc-cast bar at ThermoElectron Tecomet, Wilmington, MA. A screen wick was fabricated by wrapping four layers of 400 x 400 mesh Mo-5Re screen around a "D-shaped" mandrel. Figure 4 shows a photograph of a section of the "D-tube" and the screen wick. A 0.10-in-diameter artery was included in the wick. The artery is located in the top center of the curved portion of the heat pipe and has a spring in it to help maintain its shape. Superimposed in Figure 4 is a photograph of the closeout at one end of the wick. One end of the wick is closed out as in the photograph, while the other end is open and is covered by a pool of liquid lithium during operation. Mo-41Re end caps were machined and welded to the ends of the heat pipe. A photograph of all of the individual parts prior to the final assembly is shown in Figure 5.

After the heat pipe was assembled, Li vapor was distilled into the heat pipe. A schematic diagram of the distillation apparatus is shown in Figure 6. The distillation pot was heated by induction heating. All of the lithium was distilled into the heat pipe to insure the purity of the lithium. After the lithium was distilled into the heat pipe, the heat pipe was closed by the use of a valve.

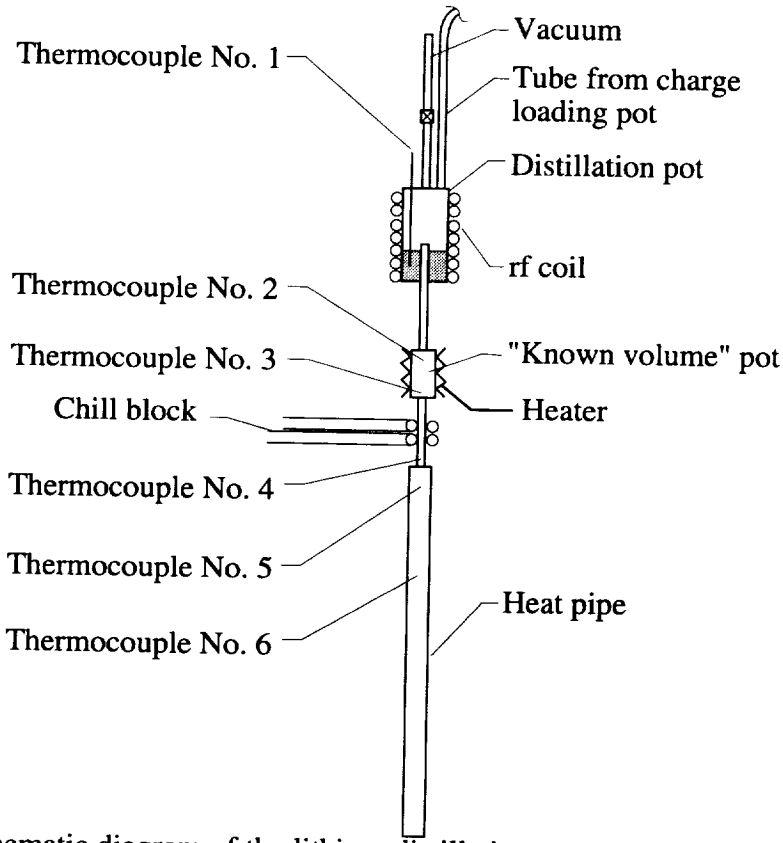

Figure 6: Schematic diagram of the lithium distillation apparatus used to charge the heat pipes.

The heat pipe was then instrumented with thermocouples. One thermocouple was located over the evaporator section end cap, while the remaining thermocouples were spaced along the condenser as shown schematically in Figure 7. A thin piece of 1/16-in. by 1/4-in. Ni foil, was spot welded to the Mo-Re heat pipe. W/W-26Re thermocouples were then spot welded to the Ni foil. The accuracy of the thermocouples is ±8°F below 800°F and ±1% above 800°F. The spot welding of the Ni foil and the thermocouples was done in an open atmosphere. All of the thermocouples were centered on the flat portion of the heat pipe.

The heat pipe was placed in a vacuum chamber with the flat side up. Water cooled cooper coils were wrapped around an approximately 4-in. length of the heat pipe near the end of the heat pipe. The heat pipe is shown in the vacuum chamber in Figure 8 (the door of vacuum chamber is removed to show the heat pipe) with the induction heating coils around the heat pipe and the thermocouples mounted on the flat surface of the heat pipe.

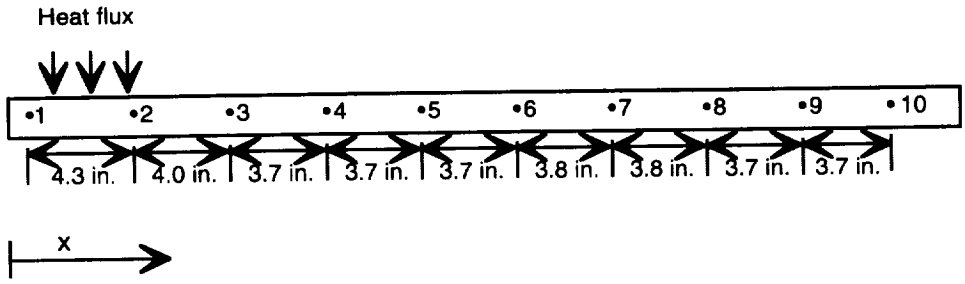

Figure 7: Schematic diagram showing the location of the thermocouples on the heat pipe.

The "D-shaped" Mo-Re heat pipe was placed in a vacuum chamber and heated by induction heating. The induction heating coils initially heated approximately 4 in. of the heat-pipe length. After several preliminary tests in which the "D-shaped" Mo-Re heat pipe was checked to ensure proper operation, the steady state throughput of the heat pipe was measured at different power supply settings. The throughput was the total integrated heat flux into the evaporator that was transferred to the condenser and radiated away by the outer surface of the heat pipe. The calorimeter that was used to determine the throughput is shown in Figure 9 along with the instrumented heat pipe. Prior to calibration, the length of the induction heating coils was reduced from 4 in. to 2 in. This reduction enabled the heat flux to be doubled while maintaining the same throughput and maximum operating temperature.

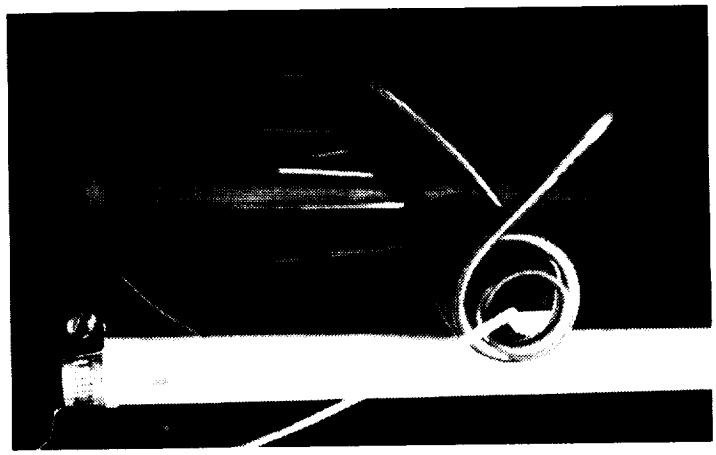

Figure 8: Photograph of the heat pipe in the vacuum chamber showing the heat pipe with thermocouples mounted on the flat surface and induction heating coils wrapped around a portion of the heat pipe.

During calibration, the heat pipe was slowly brought to a temperature of 2370°F, and steady state operation was obtained at various intermediate temperatures, as shown in Figure 10. The temperatures were monitored with both an optical pyrometer and thermocouples mounted on the heat pipe. Knowing the steady state temperature of the heat pipe, the heat radiated away (the throughput) could be related to the setting on the

power supply. The throughput for the steady state conditions are listed on the figure. However, due to the temperature dependence of the electrical resistance of the Mo-Re material, the heat input at a given power setting is different for different heat-pipe temperatures. Thus, the heat input determined from the measured throughput is not as accurate during transient conditions as during steady state operation. The heat pipe appeared to operate normally and maintained a nearly uniform temperature along its length.

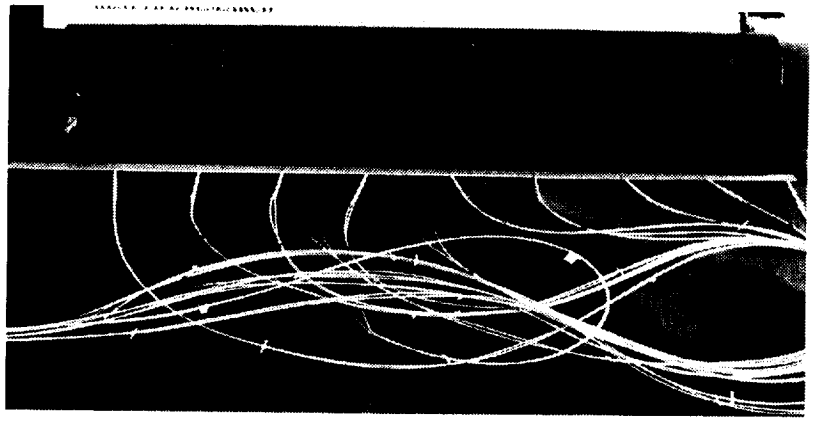

Figure 9: Photograph of the heat pipe with thermocouples and the calorimeter used to determine the throughput.

The heat pipe appeared to operate normally and maintained a nearly uniform temperature along its length. As mentioned previously, the first thermocouple was mounted over the endcap. Since it was mounted over the endcap, which was inductively heated but not cooled by the heat pipe, the first thermocouple temperature is slightly higher than the rest of the heat pipe. After the heat pipe reached a steady state temperature of ~2370°F, the power to the heat pipe was turned off and the heat pipe was allowed to cool.

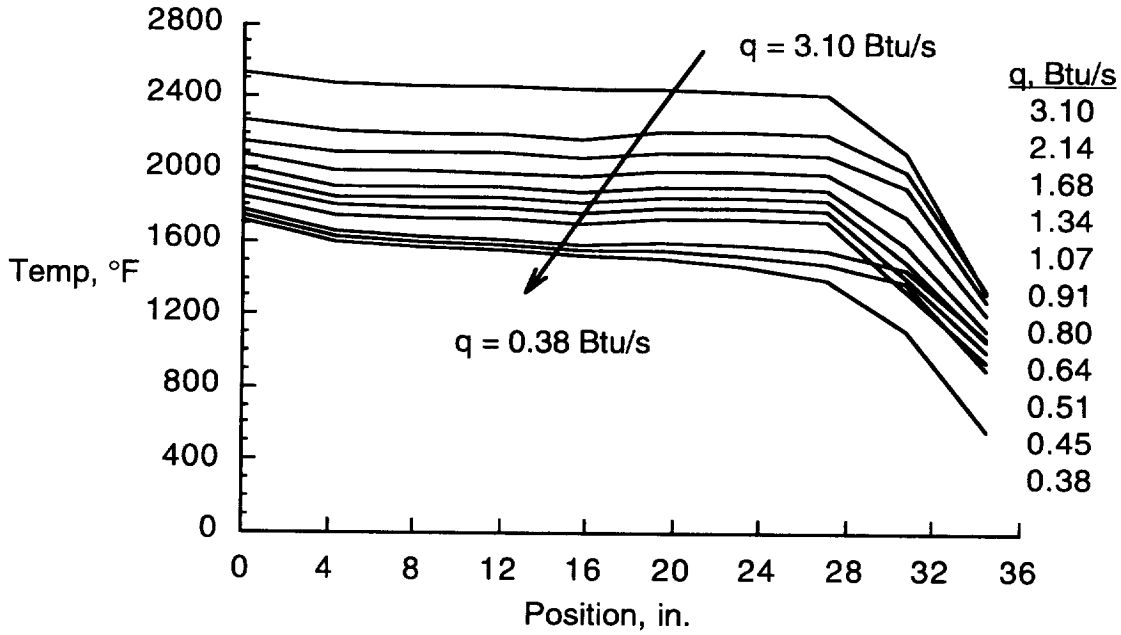

Figure 10: Steady state temperature distributions for a range of heat fluxes. (T = ±1%)

Inspection of the heat pipe after removal from the vacuum chamber indicated that several of the thermocouple wires were cracked near the location where they were welded to the Ni foil. All of the thermocouple wires were then cut off near where they were welded to the Ni foil. To hold the thermocouple wires steady and to decrease the chance of the wires cracking, the alumina insulation around the thermocouple wires was held in place with thin-gage tantalum wire. The thermocouple wires were then spot welded to the Ni foil on the Mo-Re heat pipe. The heat pipe was then placed in the vacuum chamber for subsequent induction heating.

During the heating of the heat pipe, it was noticed that the evaporator end cap of the heat pipe was much brighter in color (and thus hotter) than the remaining portion of the heat pipe. The end cap was too close to the induction heating coils, and as a result, was being inductively heated. The portion of the heat pipe directly under the induction coils, though receiving a high heat flux due to the inductive heating, was being cooled by the operation of the heat pipe. The end cap, however, was not cooled, but was inductively coupled. The heat pipe was heated to approximately 2460°F, with a heat flux in the evaporator region (under the induction coils) of 141 Btu/ft^2-s, and a throughput of 3.1 Btu/s. When the heat-pipe operating temperature reached ~2460°F, the temperature of the end cap of the heat pipe was approximately 2820°F. It was then noticed that the flat portion of the heat pipe had deformed outward, and was no longer flat. The power to the induction heaters was turned off, and the heat pipe was allowed to cool.

After the heat pipe cooled down to room temperature, it was visually inspected. The permanent deformation of the flat surface resulted in a cross-sectional thickness increase from 0.32 in. to 0.398 in. The increase in cross-sectional thickness was measured with a micrometer on the outside of the heat pipe. The deformation of the heat pipe occurred over nearly the entire length of the heat pipe. The last few inches of the condenser end of the heat pipe did not deform since it was at lower temperatures and pressures. In addition to the softening of the Mo-Re with increased temperature, the vapor pressure of the Li increases exponentially with temperature. During the initial test with the heat pipe operating at ~2370°F, the vapor pressure in the heat pipe was 11 psi and no permanent structural deformation occurred. The vapor pressure in the heat pipe during operation at ~2460°F was 16 psi. However, with an end cap temperature of ~2820°F, the local pressure in the region of the end cap was 52 psi.

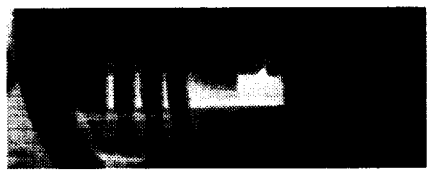

Figure 11: Photograph of the Li leak in the heat pipe.

A decision was made to continue testing the heat pipe by starting up the heat pipe with step changes in the applied heat flux occurring every two minutes. The heat pipe began to start up as expected. However, a small jet of vaporized Li was soon observed in the vicinity of the first thermocouple as shown in Figure 11. The heat pipe was operated for another 10 minutes, and then the power to the power supply was turned off. Since the heat pipe was fabricated with a small surplus of Li, and since the rate of mass loss of Li from the leak in the heat pipe was quite small, the operation of the heat pipe would not be effected until all of the surplus Li had escaped from the heat pipe. The region where the leak occurred was at thermocouple number 1. Thermocouple number 1 had been welded to the Ni foil three times, while all other thermocouples had only been welded twice. In addition, all the thermocouple spot welds were done in an open atmosphere. As mentioned previously, the temperature of the heat pipe in the region of the first

thermocouple reached 2820°F. Since the eutectic temperature of Mo and Ni is approximately 2400°F, it is likely that some melting of the heat pipe occurred. When the heat pipes are embedded in C/C, thermocouples will not be welded to the heat pipe, and heat-pipe leaks should not occur.

Though a leak occurred in the heat pipe, the heat pipe did start up from the frozen state as expected. A plot of the temperature versus time from the thermocouples is shown in Figure 12. Thermocouple number 1 is in the evaporator region near the end cap, while thermocouples 2-10 are located in the condenser region. Thermocouple number 4 is not shown on the figure since the data were in error. The sharp gradient at the thermal front can be observed in the figure from the sharp rise in temperature at a given location. The power to the heat pipe was increased at approximately 400 sec, and turned off at approximately 1000 sec.

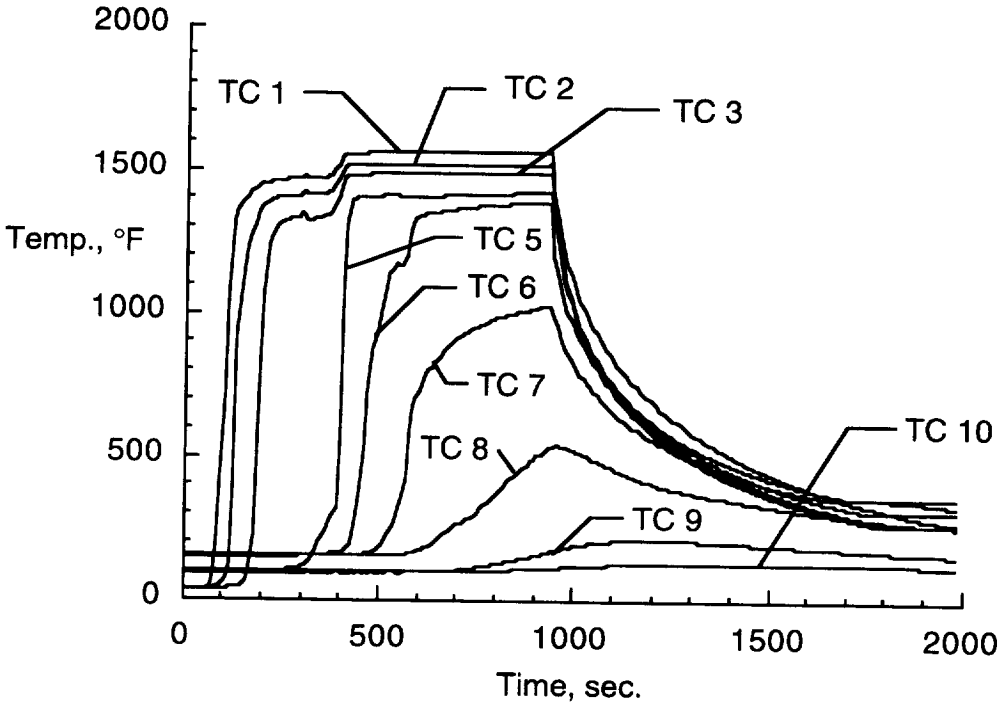

Figure 12: Temperature versus time at various thermocouple locations during start up from the frozen state of a Li/Mo-Re heat pipe. (T = ±1% above 800°F)

Two problems (deformation of the heat pipe during operation at a temperature of 2460°F and a leak at the location of a thermocouple) arose during the testing of the heat pipe. Though both of these occurrences were problematic during the testing, they should be less problematic in the actual application where the heat pipes are embedded in a C/C material, and no thermocouples are welded on the heat pipe. Prior to embedding the heat pipes in C/C, it is desirable to test the heat pipes at the operational temperature. Since the anticipated operational temperature is in the range of 2200-2300°F, the heat pipes can be tested below the temperature at which deformations are expected to occur. The above tests have also identified the need for non-welded temperature measurements for the heat pipe during start up and operation.

The greatest shortcoming of the heat-pipe tests conducted during this study was an inability to measure precisely the heat input to the heat pipe from the induction heating. The heat input to the heat pipe while operating at steady state conditions can be determined from an energy balance equating heat in and heat out. However, during start up, the heat into the heat pipe is not equal to the heat leaving the heat pipe. Since the

electrical resistance of the heat-pipe material varies as a function of temperature, the heat into the heat pipe varies during start up even with constant power settings on the power supply.

A non-linear structural finite element analysis was conducted to estimate the deformation of the heat pipe during operating conditions. A model of a "D-shaped" tube was generated using PATRAN [15] and the non-linear analysis was performed using NASTRAN [16]. Although the actual heat pipe was 36-in. long, only a 3-in-long segment of the heat pipe was modeled for the finite element analysis. The use of a 3-in-long segment in the finite element model was possible since the finite element analysis confirmed that edge effects of the end of the heat pipe were no longer present 3 in. from the evaporator end of the heat pipe. This length reduction resulted in a significant savings in computer time. The "D-shaped" tube was assumed to have a constant temperature of 2460°F, which resulted in an internal vapor pressure of 16 psi. Since the actual test was conducted in a vacuum chamber, no external pressure was applied in the finite element analysis. A solid end plug was located in the evaporator end of the actual heat pipe. The end plug was modeled in the analysis by restricting both the translations and rotations of one end of the model. Since a complete set of mechanical properties was not available for arc-cast Mo-41Re, temperature dependent stress-strain curves and a temperature dependent coefficient of thermal expansion for powder metallurgy (PM) Mo-50Re were used for most of the analysis. However, yield and ultimate stresses were available for arc-cast Mo-41Re at 2600°F, and the corresponding PM Mo-50Re stress-strain curve was modified to take into account the arc-cast Mo-41Re properties. The non-linear finite element analysis predicted an expansion of only 0.014 in. in the cross-sectional expansion of the heat pipe, as shown in Figure 13. The actual growth of the heat pipe was approximately 0.080 in. It is thought that the difference between the actual expansion of the heat pipe and the finite element analysis prediction of the expansion is due to creep.

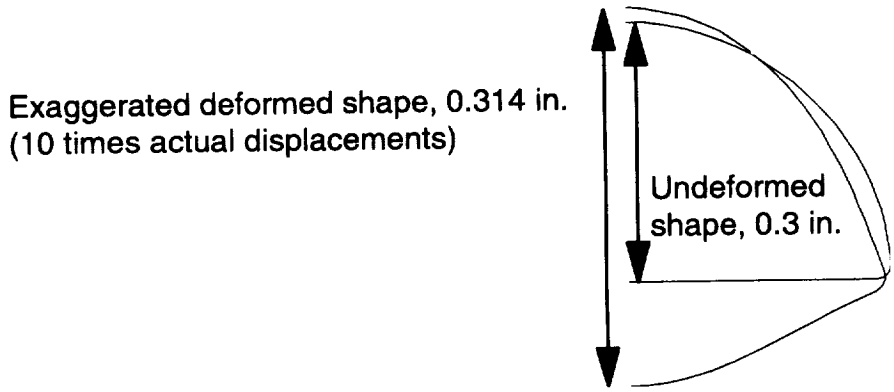

Figure 13: Schematic of undeformed and deformed shape of "D-shaped" tube from finite element analysis.

Heat Pipes Embedded in Carbon/Carbon

The leak in the design validation heat pipe was attributed to welding (in air) a thermocouple on the heat pipe in the same spot three times. However, the heat-pipe design appeared satisfactory and the heat pipe operated as expected. After the design validation heat pipe was checked out and was determined to operate as expected, it was decided to fabricate three additional heat pipes with the same design. The heat pipes

were fabricated and checked out at LANL. The heat pipes were then embedded in C/C and tested at NASA Langley Research Center.

The heat-pipe containers were initially coated with a R512E oxidation protection coating [17]. The intent was to put a coating on the heat pipes that would protect the Mo-Re from both oxidation and carbon diffusion. However, during the firing (for cleaning purposes) of the tubes at LANL, the coating began to evaporate. Due to the required purity for all heat pipe fabrication steps, an attempt was made to remove the coating so that the evaporated coating would not contaminate the heat pipe during subsequent processing. Most of the coating was removed, but as can be seen in Figure 14, not all the heat pipes appeared the same after coating removal. In the top left of the photograph is a closeup view of the end of the heat pipes with covers welded over the fill tubes.

Each heat pipe was wet in after it was charged with lithium. Heat pipe #1 was wet in for 42 hours at 1650-1740°F with 0.0099 lb of Li, heat pipe #2 was wet in for 70 hours at 1650°F with 0.0088 lb of Li, and heat pipe #3 was wet in for 47 hours at 1650°F with 0.018 lb of Li. After the wet in, each heat pipe was tested to evaluate its operation.

Heat pipe #1 was heated to a uniform temperature of approximately 2300°F. Since thermocouples were not used on the heat pipes, temperatures were estimated with an optical pyrometer. With a temperature of ~2300°F, and an induction heating coil length of 1.5 in., a heat flux of approximately 155 Btu/ft^2-s was calculated. The heat pipe was tested a second time and heated to approximately 2200°F. At this temperature, the heat pipe appeared fully isothermal with no pool at the condenser end.

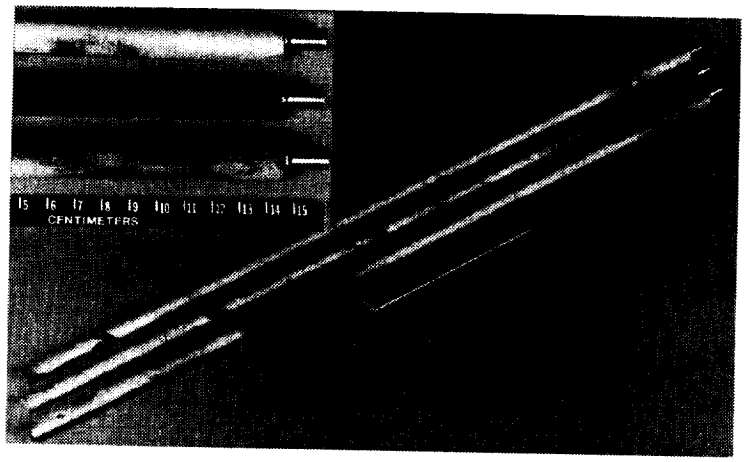

Figure 14: Photograph of the three heat pipes prior to embedding in C/C.

Heat pipe #2 was initially operated full length at ~2420°F. It was then heated a second time. Portions of the heat pipe appeared a different color than other portions of the heat pipe due to R512E coating that remained on the heat pipe. The coating modified the emittance, and thus the temperature and appearance. In the condenser section, the vapor front was not sharp, but instead consisted of ~2-in-long transition. Once the heat pipe was fully operational, it was isothermal over approximately 2 ft, with the last ~4 in. in the condenser cooler due to non condensable gas (NCG) in the heat pipe. There was a sharp transition from the isothermal portion (~1830°F) to the cooler, NCG filled region. The power to the heat pipe was increased until the temperature of the isothermal region was ~2075°F. At this point, the cool gas region at the condenser end was approximately 6-in. long.

Heat pipe #3 did not operate properly from the very beginning. A hot spot was observed on the flat surface of the heat pipe in the evaporator section (under the induction heating coils) from the beginning of the heating. The heat pipe was oriented such that the flat surface was facing upward. The heat pipe did operate full length at ~2330°F, but the hot spot remained during the entire test. The location of the heat source was moved toward the center of the heat pipe a few inches, but a hot spot remained under the coils during operation. The heat pipe was then wet in a second time at 1650°F for 72 hours. During the next test, the heat pipe started up slightly better, but a hot spot remained under the coils.

Heat pipe #3 was then tilted at an 8° angle to horizontal to assist in the flow of the liquid back to the evaporator and the induction coils were approximately 4 in. from the end of the heat pipe. The hot spot remained during testing with the condenser elevated. The hot spot spread approximately 0.5 in. on each side of the coils, slightly longer on the down hill side of the heat pipe. During heating, the hot spot remained nearly constant in size, but continued to be hotter than the rest of the heat pipe. The end plug at the evaporator also was hotter than the rest of the heat pipe. A pool of liquid lithium existed at the condenser end that was ~1.2 in. in length. Once the power was turned off, the hot spot disappeared almost immediately. The heat pipe then cooled down uniformly.

Next, an attempt was made to heat the heat pipe in the center. Heating at the opposite end was considered, but since the wick was open and covered by a pool of liquid, this option must be ruled out. The heat pipe started up without a hot spot. During start up, an operational length of ~8 in. was hot without a hot spot under the coils. When approximately 13 in. on each side of the coils was hot, the vapor front on the condenser side (side with open wick) maintained a relatively sharp appearance, while the vapor front on the evaporator side (side with closed wick) had a ~2 in. long "V" shaped transition region, as shown in Figure 15 (not to scale). Though the vapor front shape on the evaporator end was not sharp as desired, there was not a hot spot present. When the heat pipe was fully operational, a ~1-in-long pool of liquid was present at the condenser end. At the evaporator end of the heat pipe, there was an ~1-in-long section between the end of the heat pipe and the start of the "V" shaped vapor front. The non-operational end at the evaporator end was hotter than the liquid pool at the condenser end, but both were cooler than the operational portion of the heat pipe, which was ~1910°F.

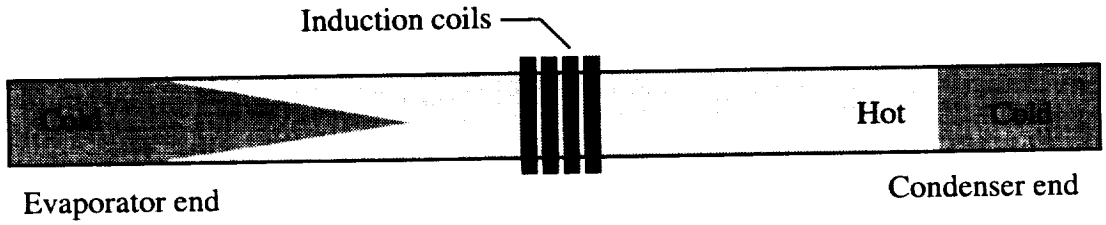

Figure 15: Schematic diagram showing the different vapor front shapes in heat pipe #3 (not to scale).

From the tests on heat pipe #3, it was determined that the most likely problem with the heat pipe was a gap between the wick and the flat surface in the evaporator end. When the region with the gap was heated, a hot spot resulted because the heat was not carried away properly by a fully wetted inner surface. When the region of the heat pipe with the gap between the flat surface and the wick was not heated directly, a cool spot resulted because of poor liquid interchange between the liquid in the gap and the rest of the heat pipe.

After the heat pipes were tested, they were all three embedded in C/C by Carbon-Carbon Advanced Technologies, Fort Worth, TX. A carbon preform was previously woven by Fiberite, Greenville, TX, with "D-shaped" channels using T-300 fibers. The fabric was heat treated at 3000°F. The heat treatment was not performed at as high a temperature as is often done because the use temperature of the heat-pipe test article is less than 3000°F and higher heat treatment temperatures result in higher modulus fibers. For the application here, the lower modulus fibers resulting from the lower temperature heat treatment is preferable. A 0.005-in-thick layer of Grafoil® (Grafoil® is a registered trademark of Union Carbide) was placed between the curved portion of the heat pipe and the carbon fibers prior to densification. This was done by bonding the Grafoil® to the heat pipes with superglue. The purpose of the Grafoil® was to serve as a compliant layer to relieve stresses due to the CTE mismatch between the Mo-Re and the C/C. A graphite tool was used in the densification process to assure proper positioning of the heat pipes. A photograph of the three heat pipes in the C/C after densification is shown in Figure 16. In the upper left corner of the photograph is a closeup view of the end of the heat pipes in the C/C.

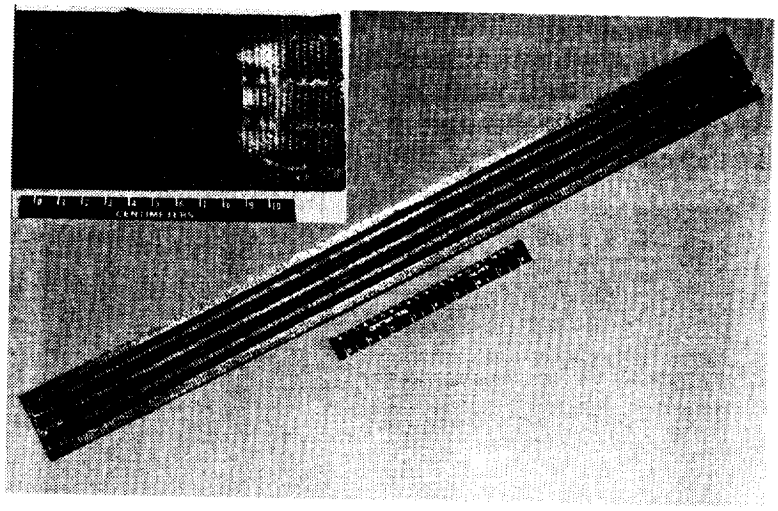

Figure 16: Photograph of the three heat pipes after embedding in C/C.

Table 1: Thermocouple Calibration

Standard thermocouple, °F	Test thermocouple, °F	Correction, °F
495.6	497.8	-2.2
997.4	1001.4	-4.0
1407.1	1411.9	-4.8
1609.2	1613.2	-4.0
1813.3	1817.4	-4.1
2019.6	2022.1	-2.5

The heat-pipe test article shown in Figure 16 was instrumented with 34 type K thermocouples. The 24 AWG wire thermocouples were sleeved with Nextel® ceramic sleeving (Nextel® is a registered trademark of 3M). The mounting procedure for the high temperature thermocouples is summarized here and detailed in Appendix A. A graphite cement from Dylon Industries was used to bond the thermocouples to the C/C. The bonding surface was lightly microblasted with 2-mil-diameter alumina at 80 psi to provide a matte surface for bonding. A precoat of 2-3 mils of the cement was then placed on the surface and allowed to air dry for 2 hours. The entire part was then heated to

260°F in air, held for 2 hours, and allowed to cool. The thermocouples were then positioned on the part and held in place with Permacel aluminum tape. The same graphite cement was then placed over the thermocouples and allowed to air dry for 2 hours. The part was then heated to 260°F in air, held for 2 hours, and allowed to cool. The aluminum tape was then removed and the final step was to heat the part in air for 2 hours at 450°F. Figure 17 shows a thermocouple mounted on the curved surface of the C/C. At the bottom of the figure can be seen eight thermocouple wires routed from the flat surface.

A thermocouple was calibrated from the same spool of wire that was used for the thermocouples bonded to the C/C. The thermocouple was calibrated in a miniature furnace with a 392 - 2012°F capability. Though test temperatures were recorded above 2000°F, the calibration could only be performed to ~2000°F. An isothermal well (Inconel/steel block with holes drilled in it) was placed in the furnace. A standard NIST calibrated type R thermocouple was inserted in one of the holes in the isothermal well and the thermocouple to be calibrated was inserted in the other hole. The other ends of the thermocouples were referenced to a 32°F ice point. At each temperature set point, a stable voltage (±1 μV) was maintained for 30 minutes prior to recording the voltage output. A HP 3457A digital multimeter was used to measure the output to within ±1 μV. ITS 90 thermocouple tables were used to convert the voltages to temperatures. The calibration curve comparing the standard NIST type R thermocouple with the type K thermocouple like those used during testing on the C/C is shown in Table 1.

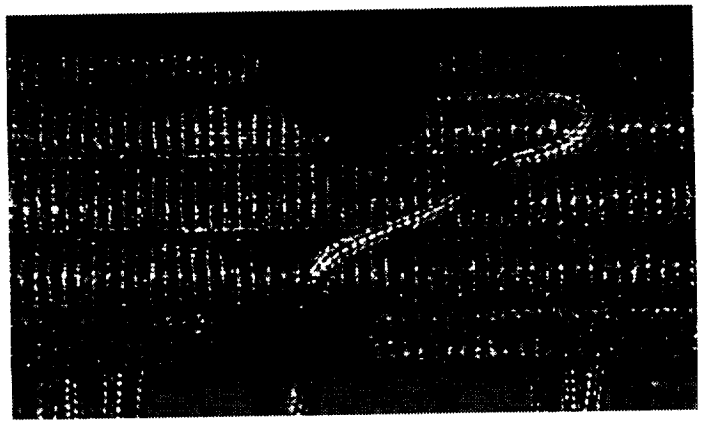

Figure 17: Photograph of thermocouple on the curved surface of the carbon/carbon.

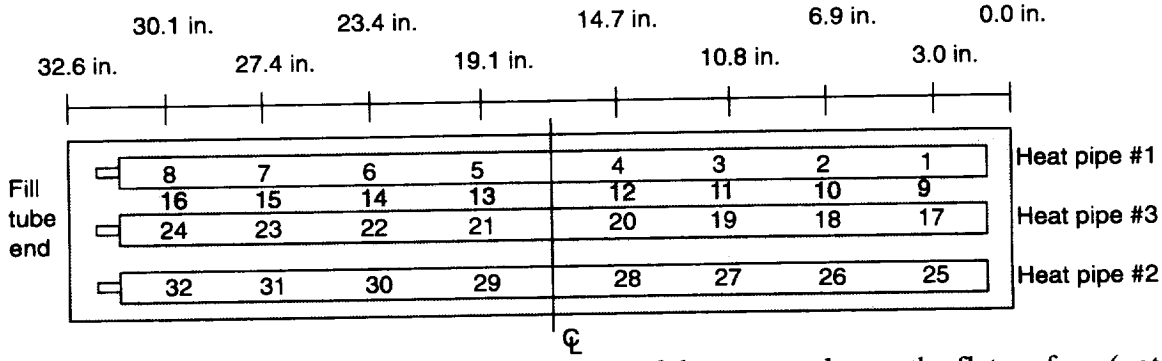

Figure 18: Schematic drawing showing location of thermocouples on the flat surface (not to scale) (x = ±1/16 in.).

As mentioned previously, 34 thermocouples were bonded to the test article. The location of the thermocouples on the flat surface are shown in Figure 18. The

thermocouple junction was under the graphite cement and thus its location was measured only to within ±1/16 in. Thermocouples No. 33 and 34 are on the side with the curved surface of the heat pipes (see Figure 17) and are located opposite thermocouples No. 3 and 6, respectively. The thermocouples are positioned such that they are centered axially on each heat pipe (TC No. 1-8, and 17-32) and in the space between two of the heat pipes (TC No. 9-16). The thermocouples are located approximately 4 in. apart except at the fill tube end of the heat pipes where the spacing is approximately 3 in.

The testing was performed in a 5 ft diameter by 5 ft long vacuum chamber at NASA Langley Research Center using quartz lamps. Prior to initiation of a test, the vacuum level was usually in the 10^{-6} torr range. During testing, the vacuum level was usually maintained in the 10^{-5} torr range, but was in the 10^{-4} torr range during times of significant outgassing.

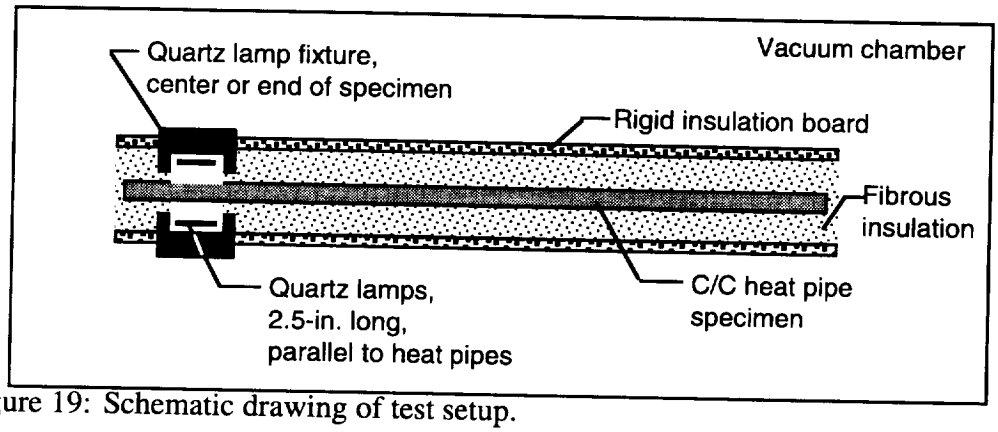

Figure 19: Schematic drawing of test setup.

A schematic drawing of the test setup is shown in Figure 19. The test article was heated either in the center or near the end, as shown in the figure. A total of twelve ~0.95 Btu/s (1 kW) quartz lamps were used, with six heating the upper surface and six heating the lower surface. The lamps, 2.5-in-long halogen cycle lamps, were oriented parallel to the heat pipes and thus the heated length of the heat pipes was 2.5 in. Four of the lamps were located over the sides of the heat-pipe test article (each side, both top and bottom), and thus did not contribute significantly to the heat flux, but did help maintain a constant heat flux across the width of the test article. Fibrous insulation and rigid insulation board were used for all except the first test to insulate the test article. The insulated test article and the heating fixtures were all placed in the vacuum chamber. (A more detailed schematic drawing of the quartz lamp heating fixture region is shown later in Figure 23).

Steady State

During the first test, the heat-pipe test article was centered under the heaters and the unheated portion was completely uncovered and radiated to the inside walls of the vacuum chamber. As a result of the radiation heat losses from the test article and the limited heat input, the heat pipes never reached operating temperatures.

From a post test evaluation of the test article, it appeared that the graphite cement attaching the thermocouples was a major source of outgassing that occurred during the test. The rows of thermocouples to the right of the centerline (TC #4, #12, #20, and #28) were located underneath the water-cooled fixture. As a result of the outgassing of the graphite cement, the fixture was much more discolored than the other side which was not located over a row of thermocouples. Cracks were evident in the graphite cement attaching the thermocouples that had been heated, but the thermocouples remained attached.

Due to the inability to heat the heat pipes to a level where they began to function as heat pipes, it was decided to insulate both surfaces of the heat-pipe test article outside of the heated zone. The test article was insulated with approximately 2 in. of ceramic insulation board as shown in Figure 20. The insulation board was baked out for approximately 2 hours at 1000°F prior to use. The photograph in Figure 20 shows the water-cooled quartz lamps fixture in the center of the test article and insulation surrounding the rest of the test article. Fibrous Saffil® (Saffil® is a trademark of Imperial Chemical Industries PLC for alumina fiber) insulation (not baked out) was placed between the C/C and the rigid insulation board since the heat-pipe test article, with thermocouples and a non-flat surface, did not conform to the flat insulation board. The Saffil® and insulation board were held in place with four pieces of stainless steel wire. Though the photograph does not show it, the heated center portion of the test article was also insulated on the sides. The heat-pipe test article was insulated and positioned in the heating fixture prior to placing the entire test apparatus in the vacuum chamber. In addition to adding the insulation, the vacuum chamber was modified by placing a large (~ 2 ft x 2 ft) cold plate in the chamber for the purpose of condensing gases resulting from outgassing. The quartz lamps were centered between the thermocouples near the middle of the test article.

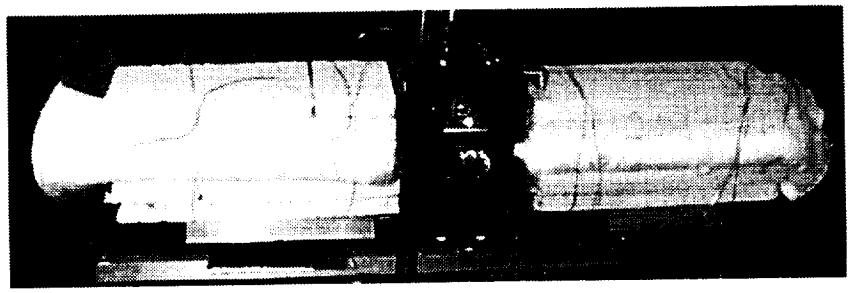

Figure 20: Photograph of the insulated C/C heat-pipe test article.

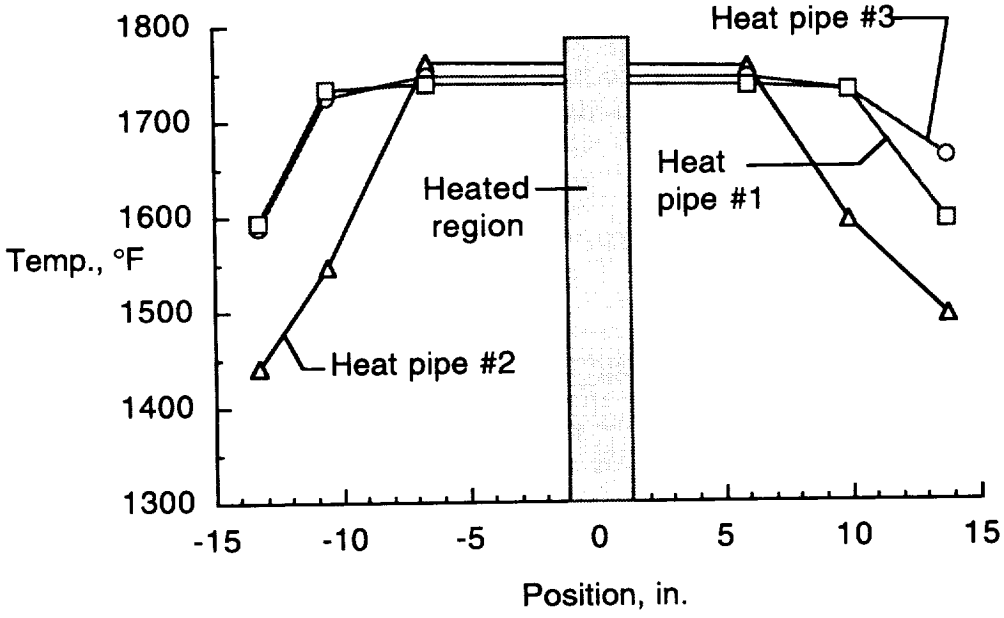

Figure 21: "Steady state" temperatures for each heat pipe (Test 2).

The test article was heated to full power over a time span of approximately 7 hours. Isothermal operation of the heat pipes was obtained, but not over the full length of the

heat pipes. The output from the quartz lamps was approximately 9.5 Btu/s (~10 kW). However, not all 9.5 Btu/s entered the C/C heat pipe test article. The "steady state" temperature distributions on the C/C over each of the heat pipes are shown in Figure 21. The term "steady state" is used, but actually, since the test article was insulated, a true steady state was not obtained. The time required to obtain true steady state conditions would be quite large. "Steady state" is used to describe the condition where only very slow increases in temperature were occurring due to the boundary effect of the insulation. The thermocouples closest to the center of the heat pipes were located underneath the water-cooled heating fixture. Due to radiation to a water cooled boundary, those thermocouples did not read meaningful temperatures and are thus not included in the figure. Heat pipes #1 and #3 were isothermal over a length greater than 20 in. Heat pipe #2 was isothermal over a shorter length than the other two heat pipes. Heat pipe #2 was not entirely isothermal during checkout of the heat pipe prior to embedding it in the C/C (see earlier section on the checkout of the heat pipes). As was mentioned earlier, it appeared that the lower temperatures on this heat pipe were due to non condensable gas (NCG) in the heat pipe.

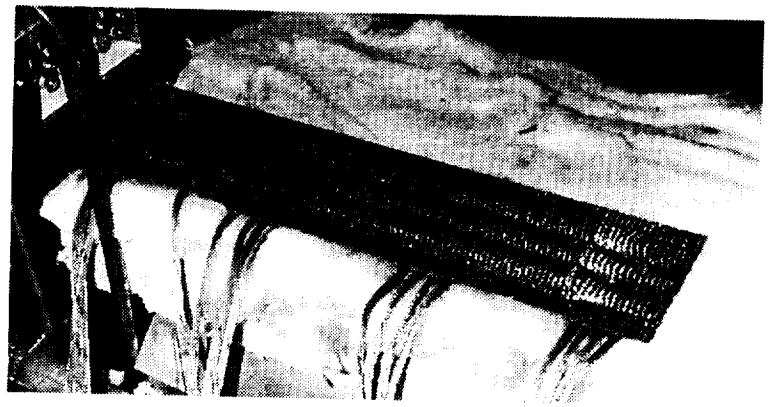

Figure 22: Photograph of the heat-pipe test article with insulation pulled back to show C/C (after Test 3).

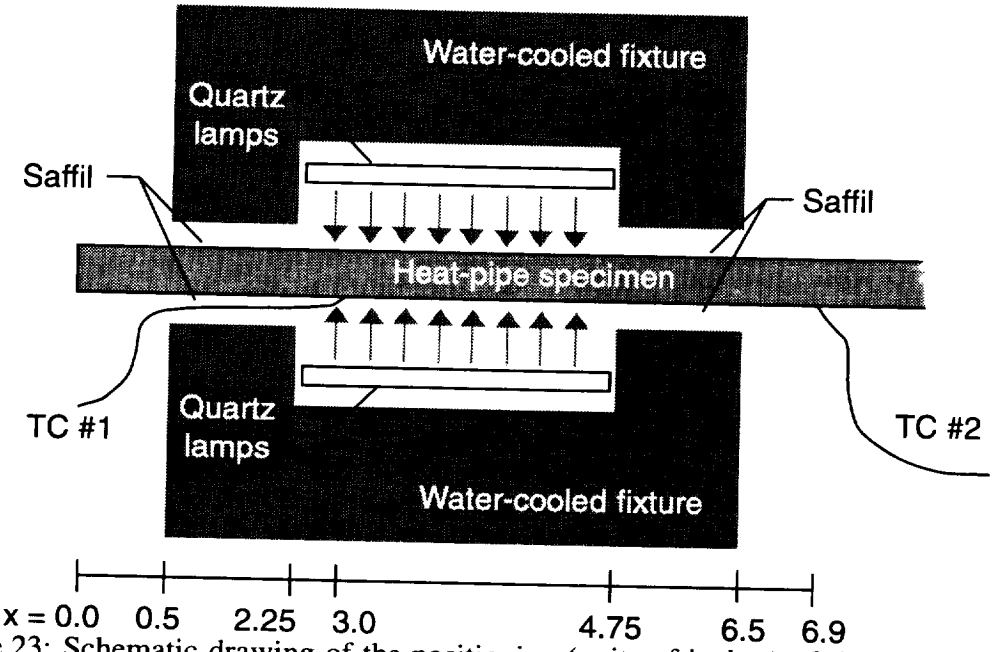

Figure 23: Schematic drawing of the positioning (units of inches) of the thermocouples relative to the water-cooled fixture (not to scale) (x = ±1/16 in.).

The heat-pipe test article was later removed from the vacuum chamber. The insulation was pulled off the test article, as shown in Figure 22, and the test article was inspected. The C/C in contact with the Saffil® insulation had a grayish tone versus the original black color. The C/C under the quartz lamps (not in contact with the Saffil®) still appeared black, and even looked slightly charred. The Saffil® insulation in contact with the C/C had a gray color, as can be seen at the top of the figure. The graphite cement mounting the thermocouples was cracked, but the thermocouples remained attached to the C/C.

The heat pipe was positioned within the heating fixture such that the heat pipe was heated at one end of the heat pipe. TC #1 (x = 2.9 in.) was located inside the heated region (2.25 in. $\leq$ x $\leq$ 4.75 in.) in order for TC #2 to be outside the heated region, as shown in Figure 23. Saffil® insulation was placed between the heat-pipe test article and the water-cooled fixture to reduce the heat loss radiated to the water-cooled fixture.

The heat-pipe test article was heated over a time period of approximately 2 hours. Figure 24 shows the temperatures at x = 23.3 in. (TC #6, #22, and #30) as a function of time. Over most of the temperature range after the heat pipes started operating, heat pipe #2 was significantly cooler than heat pipes #1 and #3. However, once the higher temperatures were reached, heat pipe #2 temperatures experienced a sudden increase to the range of the other two heat pipes.

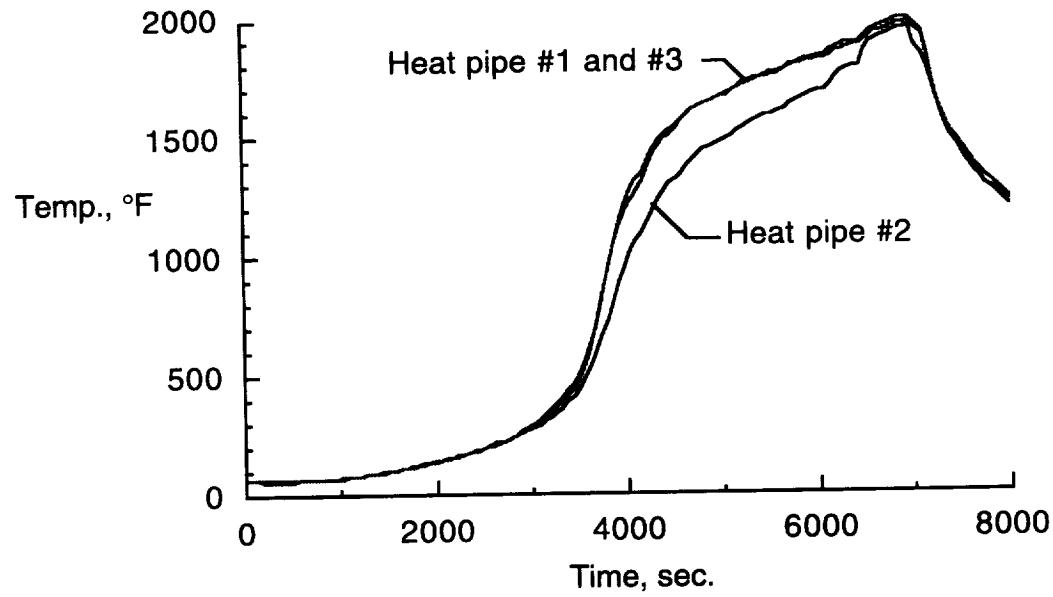

Figure 24: Temperatures at x = 23.3 in. (TC #6, #22, and #30) as a function of time for each of the three heat pipes (Test 5).

After a few minutes at the maximum heat flux attainable with the quartz lamps, one of the quartz lamps failed and the test was stopped. Figure 25 shows the temperatures at the maximum heat flux levels just prior to the bulb failure. The temperatures were not yet steady state as they appeared to be slowly increasing. The temperature of the thermocouples under the quartz lamps are also shown in Figure 25.

Temperature distributions on the C/C over each of the three heat pipes are shown in Figure 26 at two different heat flux levels. The dashed lines represent the "steady state" temperatures with a voltage of 130 V. The "steady state" temperatures represented by the solid lines are with a voltage of 180 V. The first thermocouple outside of the heated

region on heat pipe #1 (TC #2) was not operating properly and is thus not shown on the figure. Heat pipes #1 and #3 were relatively isothermal over a significant length of the test article, with heat pipe #3 isothermal over a slightly longer length. Heat pipe #2, however, again demonstrated less capability than heat pipes #1 or #3. At the 130 V level, heat pipe #2 was isothermal over a shorter length than the other two heat pipes. At the 180 V level, heat pipe #2 temperatures were still lower than those of the other two heat pipes, and appeared to have a dome-shaped distribution. This is unlike the temperature distribution shown in Figure 25.

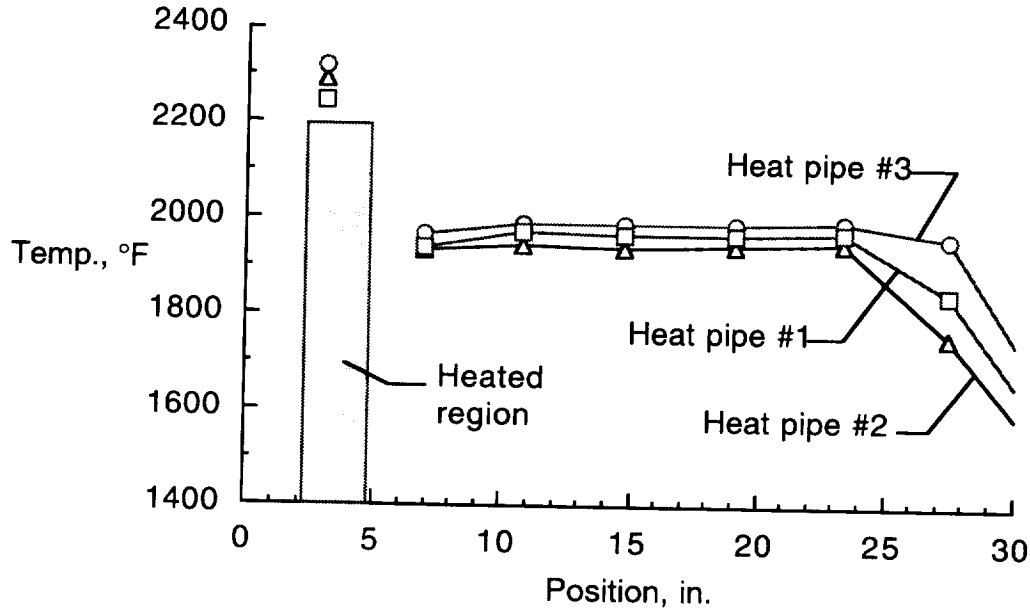

Figure 25: "Steady state" temperatures for each heat pipe in the horizontal orientation (Test 5).

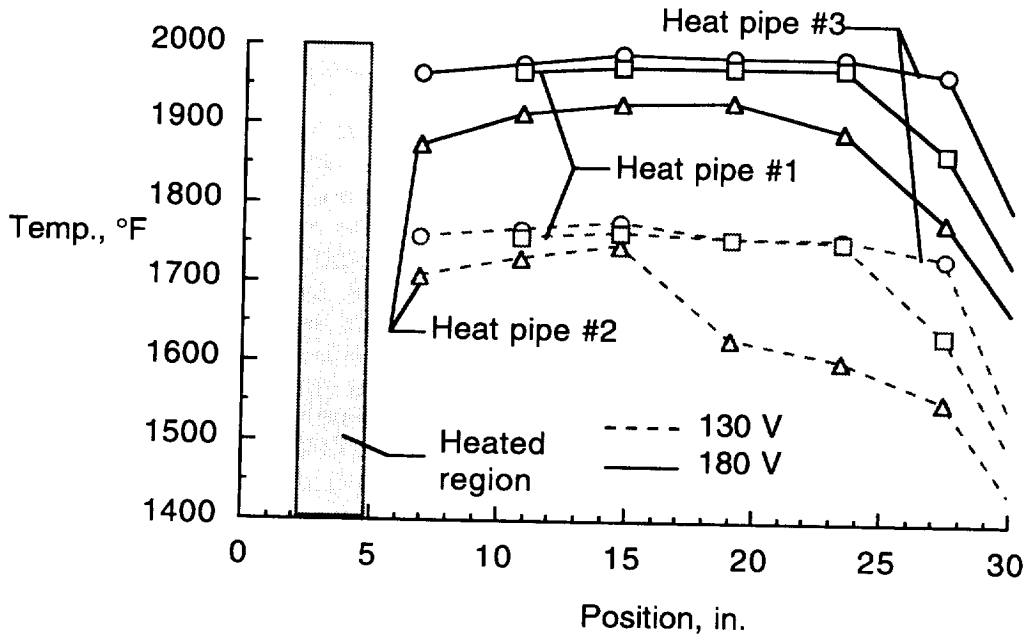

Figure 26: Heat-pipe-temperature (on C/C) distributions in the horizontal orientation (Test 6).

After a "steady state" condition had been maintained at 130 V, the voltage was increased to 180 V. Figure 27 shows the transient temperature from each of the thermocouples over heat pipe #3 prior to and after the increase in voltage. The two thermocouples furthest from the heaters at x = 27.4 in. and x = 30.0 in. are labeled in the figure. The temperatures at the remaining locations were relatively isothermal and are not labeled. As can be seen in Figure 27, the temperatures along the entire length of the heat pipe (even at x = 30.0 in.) increase together. This type of behavior is to be expected for a heat pipe. However, for heat pipes embedded in C/C, differences in thermal resistance (such as contact resistance) would result in different rise times for the temperatures at different locations. Thus the results shown in Figure 27 indicate that the thermal resistance between the heat pipe and the C/C was consistent along the entire length of the test article.

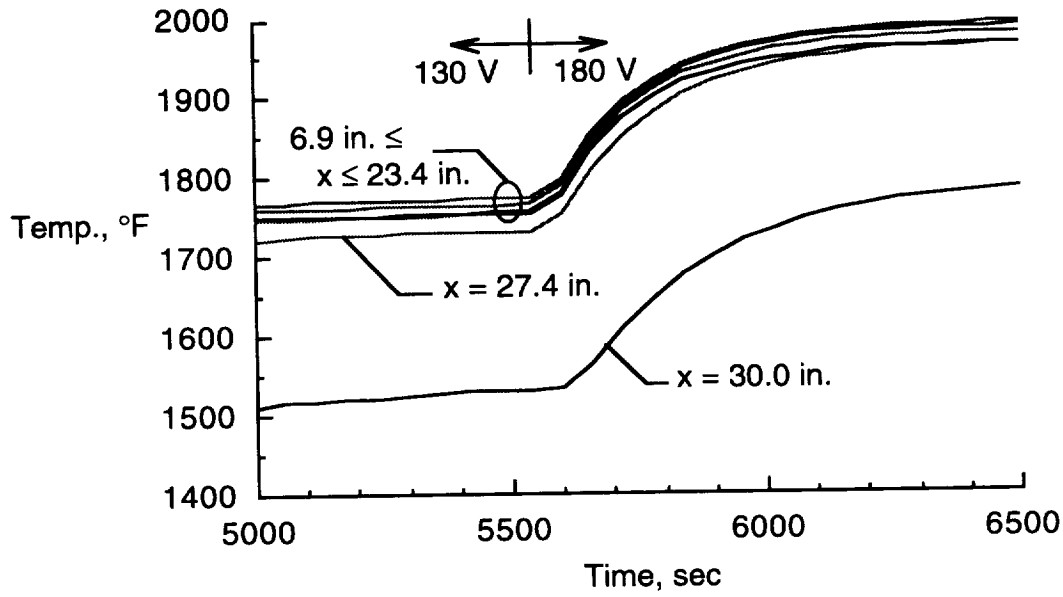

Figure 27: Temperature distribution while transitioning from one steady state condition to another steady state condition in the horizontal orientation (Test 6).

Though most of the testing was performed in the horizontal orientation, testing was also performed with the heat pipes vertical, heated at the top. The test rig with the heater at the top and insulated heat pipe used for the vertical testing are shown in Figure 28. The "steady state" temperature distribution for each of the heat pipes in both the vertical and horizontal orientation is shown in Figure 29. The voltage was 180 V in both tests. Heat pipe #2 had a dome-shaped temperature distribution, with the temperatures near the heated region lower than those near the center of the heat pipe. The temperatures of the vertical heat pipes were slightly higher than the horizontal heat pipes near the heated region. However, at the condenser end of the heat pipes, the vertical heat-pipe temperatures were significantly lower than the horizontal temperatures. Though the voltage to the quartz lamps was the same in both tests, different amount of outgassing products collected on the quartz lamps reflector or slightly different insulation geometry around the heat pipes may have had an influence on the heat-pipe temperatures. In both tests, the thermocouples in the heated regions indicated similar temperatures, indicating that the heat input was not significantly different.

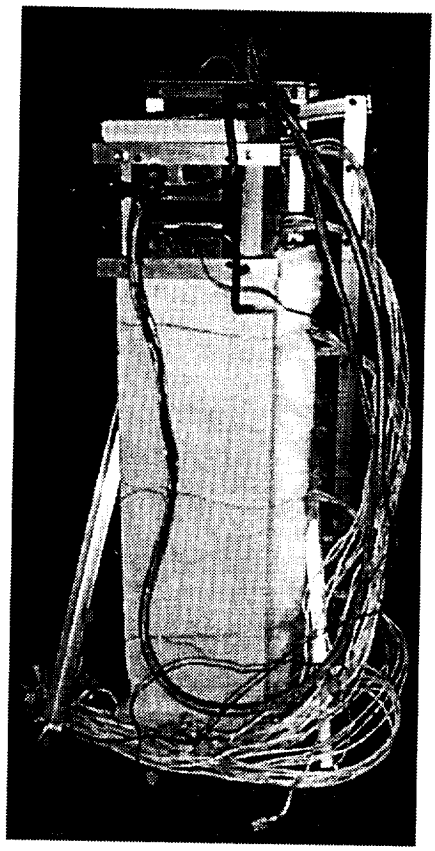

Figure 28: Photograph of the test rig and insulated heat pipe for vertical testing.

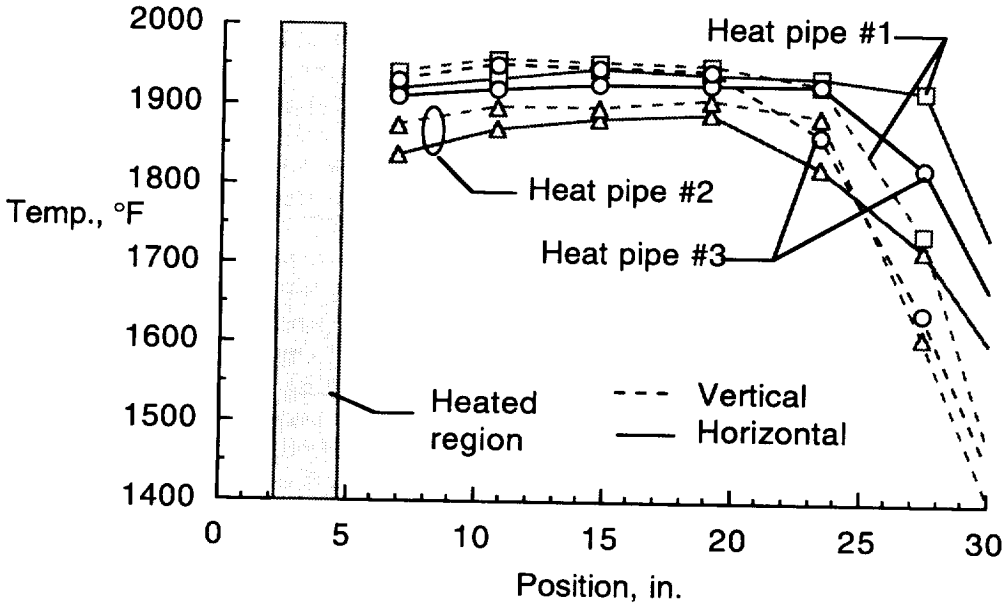

Figure 29: Comparison of "steady state" temperature distributions (180 V) over each heat pipe in both the vertical and horizontal orientation (Test 7&10).

Startup From The Frozen State

Start-up of the heat-pipe test article was performed over a time of 30 min. with the heat pipes in both the vertical and horizontal orientations. The voltage to the quartz lamps was increased to 180 V in six unequal steps. The voltage was maintained at the maximum level of 180 V until a relatively steady state was obtained.

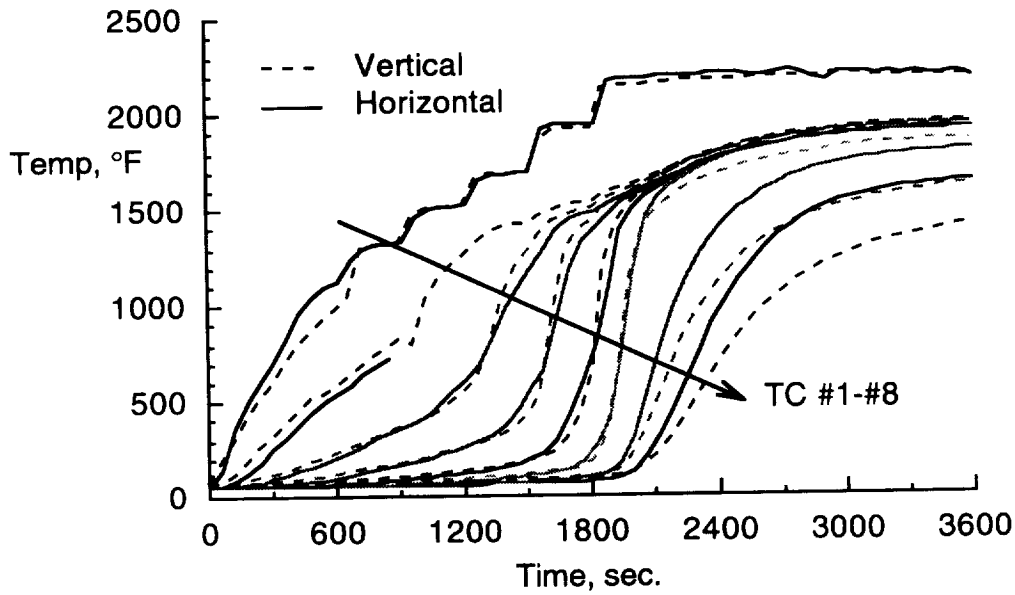

Figure 30: Start-up temperature distributions on heat pipe #1 in the horizontal and vertical orientation.

The transient temperatures over heat pipe #1 in both orientations are shown in Figure 30 for each of the eight thermocouples. The solid lines represent the horizontal orientation and the dashed lines represent the vertical orientation. The first thermocouple (TC #1) was located under the quartz lamps and thus responded much quicker and experienced higher temperatures. Though some difference can be seen in the horizontal and vertical temperatures under the heaters (TC #1), they are similar, indicating similar heat inputs. The thermocouple next to the heated region (TC #2) did not operate properly during a portion of the horizontal test. As a result, its temperatures are shown only during the early stages of the test. The sharp increase in temperatures as the heat-pipe operating length increased down the length of the heat pipe can be seen. At "steady state", the heat pipe was operating isothermally over a greater length in the horizontal orientation than in the vertical orientation. However, during the startup, the horizontal and vertical heat-pipe temperatures were similar. It was only at the higher heat fluxes and at the condenser end of the heat pipes that the vertical heat-pipe temperatures began to lag the horizontal heat-pipe temperatures. Away from the condenser end of the heat pipe, as the heat pipe was starting up, the temperature rise was steeper for the vertical heat pipe than the horizontal heat pipe. This can be observed by noting that the vertical heat-pipe temperature rise starts after the horizontal heat-pipe temperature rise, but levels off prior to the horizontal heat-pipe temperatures.

The temperatures over heat pipe #3, the center heat pipe in the test article, can be seen in Figure 31 in both the horizontal and vertical orientation. The thermocouple next to the heated region (TC #2) did not operate properly during a portion of the horizontal test. As a result, its temperatures are shown only during the early stages of the test. The temperatures are similar to those in Figure 30, except that the isothermal length was

slightly longer. Figure 32 shows the temperatures over heat pipe #2 during the start up. Heat pipes #1 and #2 were on the sides of the test article, sandwiching heat pipe #3 between them. That may contribute to the fact that the middle heat pipe (heat pipe #3) was, in general, isothermal over a longer length than either of the two heat pipes on the sides.

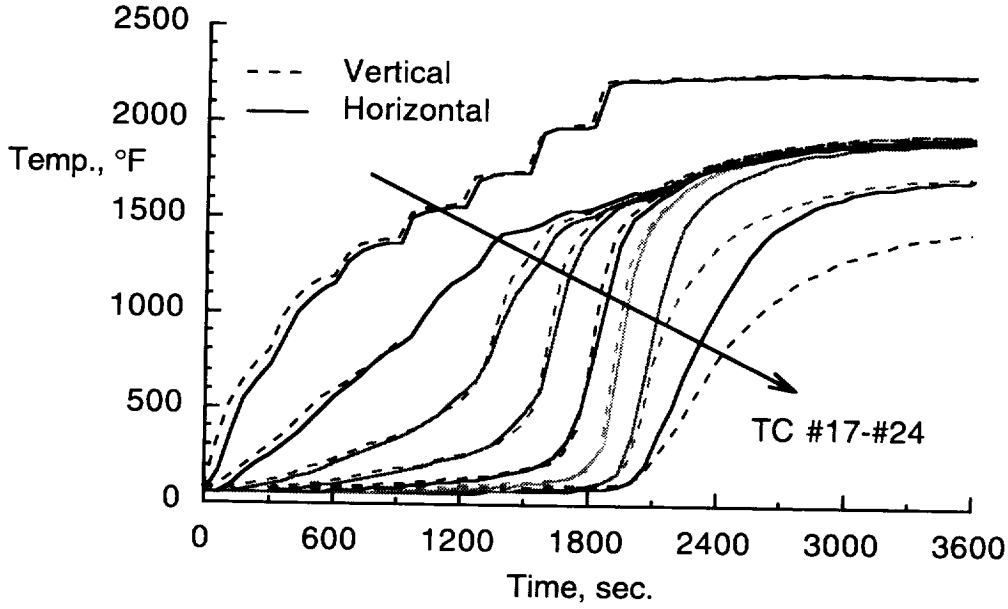

Figure 31: Start-up temperature distributions on heat pipe #3 in the horizontal and vertical orientation.

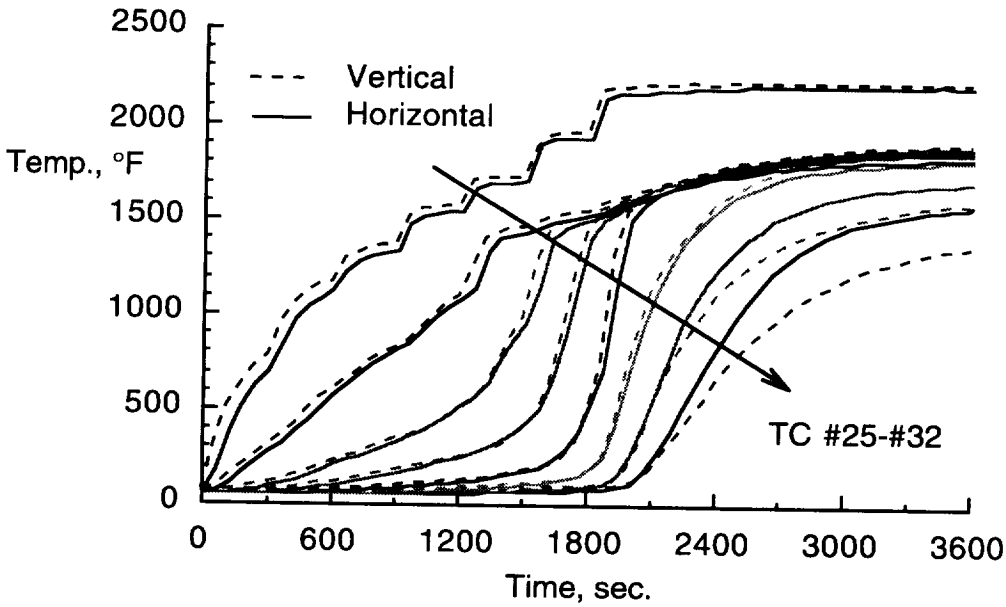

Figure 32: Start-up temperature distributions on heat pipe #2 in the horizontal and vertical orientation.

Each of the heat pipes had a 5-mil-thick sheet of Grafoil® between the heat pipe and the C/C on the curved surface of the heat pipe. On the flat surface, which is the heated surface on an actual leading edge, no Grafoil® was used in an effort to minimize the

thermal resistance. Figure 33 shows the transient temperatures at x = 10.8 in. and x = 23.3 in. on both the flat (no Grafoil®) and curved (with Grafoil®) surfaces with the heat pipes in the horizontal orientation. At x = 10.8 in., the temperature of the surface with no Grafoil® increased faster than the surface with Grafoil® between the heat pipe and the C/C. That was as expected since the Grafoil® should result in increased thermal resistance. However, at x = 23.3 in., the surface with no Grafoil® between the C/C and the heat pipe increased slower than the surface with the Grafoil®. The difference in thermal response at the two locations was also present in other horizontal tests and with the heat pipes in the vertical orientation.

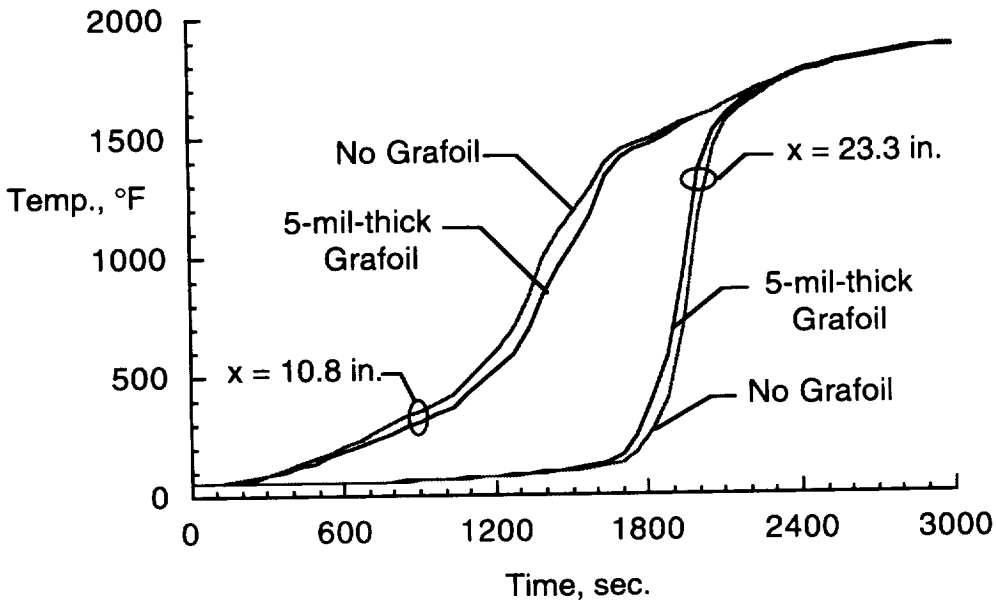

Figure 33: Comparison of temperature rise with and without 5-mil-thick Grafoil® between heat pipe #1 and the C/C with the heat pipe in a horizontal orientation (Test 7).

Non Destructive Evaluation

Non destructive evaluation of the C/C heat-pipe test article was performed prior to testing and after testing. Prior to testing, radiography was performed on the as fabricated test article. Figure 34 shows an X-ray of the heat pipes embedded in the C/C prior to testing. Arteries, with outer diameters measured between 0.135 in. and 0.160 in. (design diameter of 0.1 in.), can be seen in each heat pipe. Due to the angle of the X-ray, the arteries (centered at the top, curved portion of the heat pipe) appear not to be located in the center of the heat pipes. The straight heat pipes also appear to be curved, though they are straight. The X-ray revealed several areas of lower density, as indicated in the figure. The lower density areas result in less X-ray attenuation, and thus darker images. The thinner tube cross sections could be the result of the tube drawing or the sandblasting removal of the R512E coating.

Additional radiography was performed on the heat pipes after testing. The distance between the heat pipes was measured from the X-rays, and found to be slightly different between different heat pipes. The distance between the heat pipes varied along the length, but was approximately 0.075 in. and 0.085 in. One gap was noticeably (~0.010 in.) wider than the other gap. The spacing was to have been 0.040 in, indicating that the gaps were approximately twice the design gap.

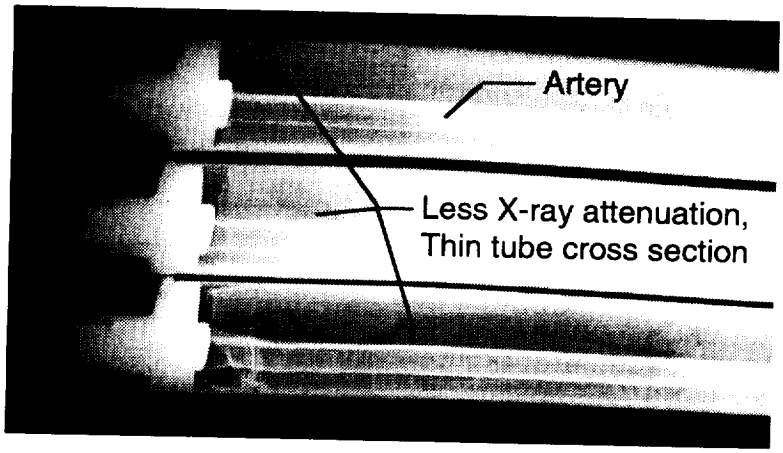

Figure 34: X-ray of the three heat pipes embedded in C/C showing the arteries in the heat pipe and areas of less attenuation.

Figure 35 shows a side view X-ray of the C/C heat-pipe test article. The test article was aligned with a laser prior to the radiography. This alignment helped to obtain as accurate a reading as possible for the C/C thickness. However, the thickness measurement is still only an estimate. From this view, the thickness of the C/C over the heat pipes was estimated to be ~0.035 in. This thickness compares favorably with the design thickness of 0.040 in. Any misalignment between the X-ray and the flat surface of the tubes would increase the C/C thickness, thus implying a C/C thickness of at least 0.35 in.

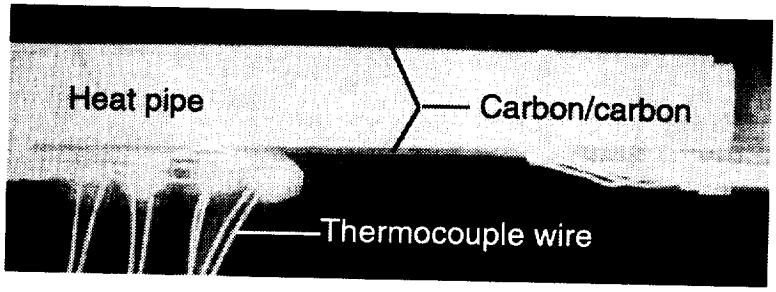

Figure 35: Side view X-ray of the heat-pipe test article on end showing the thermocouple wires and the C/C embedding the heat pipes.

Eddy current "lift-off" thickness tests were also performed on both the flat and curved surface of the C/C. The eddy current measurements provide more accurate thickness data than the visual measurement from the X-ray. A 100 kHz EM6300 tester was used with an unsupported pancake probe. Table 2 lists the results from the eddy current tests. The values in the table are the thickness of the C/C on the flat surface and the C/C and Grafoil® on the curved surface. Any gaps would also be included in the thickness measurements. The different thicknesses may also be due to irregularities in processing or tooling. It is uncertain what the effect of the screen wick is on the thickness measurements. However, the screen is uniform over the entire length and would contribute at most 0.002 - 0.003 in. to the overall thickness.

Figure 36 graphically shows the thicknesses along the length of each heat pipe. As in Table 2, the thickness of the container is not included. A disbond, or gap, appears to be present on the flat surface of the center heat pipe (HP #3) at locations x = 3 3/4 in. and x = 7 1/2 in. This hypothesis is based on both the larger thickness and the sound generated by tapping on the C/C. On the same heat pipe, at x = 17 in. and x = 22 1/4 in., the sound

generated by tapping did not indicate a disbond. On the curved surface of heat pipe #1 at x = 30 in, tapping on the C/C indicated a potential disbond.

Table 2: Eddy Current "Lift-off" Test Thickness

Curved surface, in.				Flat surface, in.			
x	HP #1	HP #3	HP #2	x	HP #1	HP #3	HP #2
3	0.049	0.053	0.052	3 3/4	0.045	0.058	0.048
5	0.049	0.053	0.052	7 1/2	0.045	0.058	0.048
10	0.053	0.053	0.054	11 1/2	0.043	0.050	0.047
15	0.053	0.055	0.051	17	0.042	0.058	0.048
20	0.051	0.054	0.052	22 1/4	0.043	0.059	0.049
25	0.054	0.055	0.053	26 1/4	0.042	0.050	0.047
30	0.062	0.053	0.055				

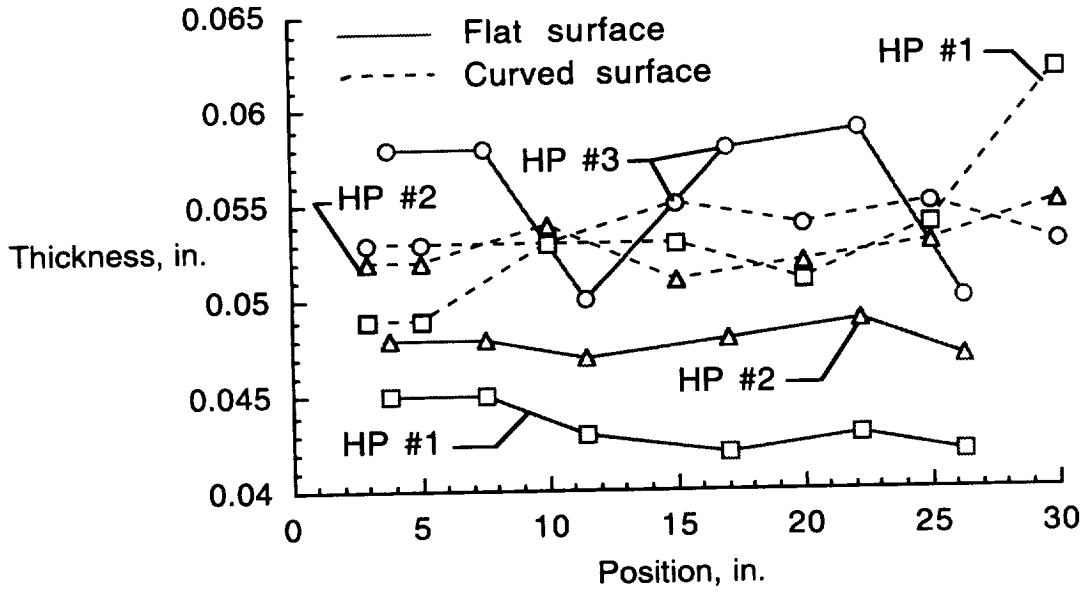

Figure 36: Plot of thickness data (less heat-pipe container) from eddy current tests.

During testing, heat pipe #1 appeared to operate the best and have consistently high steady state temperature distributions. That is consistent with Figure 36, which indicates the thinnest C/C is over the flat surface of heat pipe #1. However, for heat pipes #2 and #3, the thickness and temperatures did not always correlate. This may be due to the differences in the heat-pipe operation, i.e., presence of NCG, or from the fact that the entire test article was insulated.

Both the thickness of the C/C and the distance between heat pipes was larger in the actual test article than in the design. One technique to approach the design thickness and heat-pipe spacing is to put additional Grafoil® on the curved surface between the heat pipe and the C/C. The additional Grafoil® would "tighten up" the carbon preform since the insert (heat pipe and Grafoil®) would be larger. The effect would be thinner C/C and closer spaced heat pipes.

Concluding Remarks

The fabrication of a heat-pipe-cooled leading edge for hypersonic vehicles has moved from the preliminary design stage to the fabrication and testing of several sub-components. The present paper discusses several heat pipes that were fabricated and tested toward this goal.

A Mo-Re "D-shaped" heat pipe was fabricated and successfully operated up to a temperature of 2460°F. However, at that temperature, the flat side of the heat pipe deformed due to the internal pressure. The heat pipe was subsequently started from the frozen state and it operated as expected. A leak was observed at the location of a thermocouple which had been spot welded three times in an open atmosphere. Though both of these occurrences were problematic during the testing, they would not be problematic in actual applications where the heat pipes are embedded in a C/C material, and no thermocouples are welded on the heat pipes.

In addition to testing the single heat pipe, three additional heat pipes were fabricated and embedded in C/C. The successful operation of each of these heat pipes was determined prior to embedding in C/C. The C/C test article with the three heat pipes was tested with quartz lamps in a vacuum chamber in both a horizontal and vertical orientation. Insulation was required around the entire test article to reduce heat losses in order for the heat pipes to operate properly. All three heat pipes operated successfully, but each performed differently. The heat pipes were started up successfully from the frozen state numerous times. Both start up and steady state data are presented.

The tests demonstrated that heat pipes can be embedded in C/C and successfully operated. Though the contact resistance across the interface between the heat pipe and the C/C was unknown, it was not thought to be significant based on relatively uniform surface temperatures. However, insulating the test article could also contribute to the relatively uniform temperatures. The non destructive evaluation performed after testing indicated differences in the C/C thickness. One potential disbond area was identified, but many of the thickness variations may be due to processing or tooling irregularities.

Acknowledgments

The authors would like to thank NASA Langley Research Center for funding this work under contract No. NAS1-96014. The authors would also like to thank Robert Ortega (LANL), Joe Sikora (NASA LaRC), and Jeff Knutson (NASA LaRC) for their assistance in testing the heat pipes.

References

1. Silverstein, C. C.: A Feasibility Study of Heat-Pipe-Cooled Leading Edges for Hypersonic Cruise Aircraft. NASA CR 1857, 1971.
2. Niblock, G. A.; Reeder, J. C.; and Huneidi, F.: Four Space Shuttle Wing Leading Edge Concepts. Journal of Spacecraft and Rockets, Vol. 11, No. 5, May 1974, pp. 314-320.
3. Alario, J. P.; and Prager, R. C.: Space Shuttle Orbiter Heat Pipe Application. NASA CR-128498, 1972.
4. Anon.: Study of Structural Active Cooling and Heat Sink Systems for Space Shuttle. NASA CR-123912, 1972.
5. Anon.: Design, Fabrication, Testing, and Delivery of Shuttle Heat Pipe Leading Edge Test Modules. NASA CR-124425, 1973.
6. Camarda, Charles J.: Analysis and Radiant Heating Tests of a Heat-Pipe-Cooled Leading Edge. NASA TN D-8468, August 1977.

7. Camarda, Charles J.: Aerothermal Tests of a Heat-Pipe-Cooled Leading Edge at Mach 7. NASA TP-1320, November 1978.
8. Camarda, Charles J.; and Masek, Robert V.: Design, Analysis and Tests of a Shuttle-Type Heat-Pipe-Cooled Leading Edge. Journal of Spacecraft and Rockets, Vol. 18, No. 1, January-February, 1981.
9. Peeples, M. E.; Reeder, J. C.; and Sontag, K. E.: Thermostructural Applications of Heat Pipes. NASA CR-159096, 1979.
10. Boman, B. L.; Citrin, E. C.; Garner, E. C.; and Stone, J. E.: Heat Pipes for Wing Leading Edges of Hypersonic Vehicles. NASA CR-181922, January 1990.
11. Boman, B.; and Elias, T.: Tests on a Sodium/Hastelloy X Wing Leading Edge Heat Pipe for Hypersonic Vehicles. Presented at the AIAA/ASME 5th Joint Thermophysics and Heat Transfer Conference, June 18-20, 1990, Seattle, WA. AIAA Paper 90-1759.
12. Colwell, Gene T.; Jang, Jong H.; and Camarda, Charles J.: Modeling of Startup from the Frozen State. Presented at the Sixth International Heat Pipe Conference, Grenoble, France, May 25-29, 1987.
13. Glass, David E.; and Camarda, Charles J.: Preliminary Thermal/Structural Analysis of a Carbon-Carbon/Refractory-Metal Heat-Pipe-Cooled Wing Leading Edge. AIAA Progress in Astronautics and Aeronautics, "Thermal Structures and Materials", Vol. 140, 1992.
14. Glass, D. E.; Camarda, C. J.; Merrigan, M. A.; Refractory-Composite/Heat-Pipe-Cooled Leading Edge, U.S. Patent No. 5,720,339, February 24, 1998.
15. Anonymous: PATRAN Users Manual, Version 3.0, PDA Engineering, 1993.
16. Lee, Sang H., editor: MSC/NASTRAN Handbook for Nonlinear Analysis, Version 67, The MacNeal-Schwendler Corporation.
17. Glass, D. E: Oxidation and Emittance Studies of Coated Mo-Re, NASA CR 201753, October 1997.

Appendix A: Surface Preparation and Installation of High-Temperature Thermocouples

Installation Materials

1. Thermocouple, type: "K", Omega part No. XC-K-24 (AWG #24, lead wire length will be determined by the test set-up requirements)
2. Thermocouple connectors, type: "K", Omega part No. NMP-K-MF (includes male & female connector pairs)
3. Thermocouple junction and leadwire hold-down cement, type: Dylon, Grade GC Cement

Surface Preparation

1. After determining the exact locations for the thermocouple junctions and the lead wire routing along the surface of the test article, spots for securing the junction and the wiring to the surface should also be determined.
2. Mask and micro-sandblast these spots with 2-mil diameter Al_2O_3 abrasive powder.
3. Remove the masking tape and eliminate any sandblast residue using clean, dry shop air. Note: When this ceramic cement is to be applied to an uncoated carbon/carbon test article, the test article must first be dried by heating it to 225°F and holding it at that temperature for one hour.
4. Once the test article is dry and at room temperature, apply a basecoat of the Dylon GC cement to all micro-sandblasted spots on the test article surfaces. This coating should be kept as thin as possible, i.e., approximately 0.002-in. to 0.003-in. thick.
5. Allow the basecoat to air dry for two hours. Then, place the test article, with the basecoated spots, in a temperature chamber and slowly raise the temperature to 275°F and hold the test article at this temperature for 2 hours. The temperature rise should not exceed 4°F/minute.

Installation

1. Once the basecoat has been cured, place the thermocouple lead wires along the predetermined routes of the test article surfaces with the thermocouple junctions appropriately positioned. The thermocouple junctions and their lead wires should now be taped down adjacent to the basecoat spots. Permacel brand aluminum tape works well.
2. Next, apply a coat of the Dylon GC cement over the thermocouple junctions and lead wires at the previously precoated spots. Note: It is important to maintain a low profile with the ceramic cement. Keep the amount of cement over the thermocouple lead wires and junctions at a minimum.
3. Allow the cement to air dry for 2 hours.
4. Place the test article in the temperature chamber and slowly raise the temperature of the test article to 275°F. Hold the test article at this temperature for 2 hours. The temperature rise should not exceed 4°F/minute.
5. Cool the test article and inspect the bonded areas making certain that there are no micro-cracks or debonding of the cement. The test article is now ready for final curing.
6. Final curing is achieved by placing the test article in the temperature chamber and slowly raising its temperature to 450°F. Hold the test article at this temperature for 2 hours.
7. Finally, cool the test article and perform a final inspection. The thermocouple installations should now be ready for service to test temperatures of 2500°F.

REPORT DOCUMENTATION PAGE

Form Approved OMB No. 0704-0188

1. AGENCY USE ONLY (*Leave blank*)	2. REPORT DATE	3. REPORT TYPE AND DATES COVERED
	March 1998	Contractor Report

4. TITLE AND SUBTITLE
Fabrication and Testing of Mo-Re Heat Pipes Embedded in Carbon/Carbon

5. FUNDING NUMBERS
NAS1-96014
WU 242-33-03-20

6. AUTHOR(S)
David E. Glass, Michael A. Merrigan, and J. Tom Sena

7. PERFORMING ORGANIZATION NAME(S) AND ADDRESS(ES)
Analytical Services & Materials, Inc.
107 Research Drive
Hampton, VA 23669-1340

8. PERFORMING ORGANIZATION REPORT NUMBER
AS&M-LS05-98-01

9. SPONSORING/MONITORING AGENCY NAME(S) AND ADDRESS(ES)
National Aeronautics and Space Administration
Langley Research Center
Hampton, VA 23681-2199

10. SPONSORING/MONITORING AGENCY REPORT NUMBER
NASA/CR-1998-207642

11. SUPPLEMENTARY NOTES
Langley Technical Monitor: Steven J. Scotti

12a. DISTRIBUTION/AVAILABILITY STATEMENT
Unclassified-Unlimited
Subject Category 34 Distribution: Nonstandard
Availability: NASA CASI (301) 621-0390

12b. DISTRIBUTION CODE

13. ABSTRACT (*Maximum 200 words*)
Refractory-composite/heat-pipe-cooled wing and tail leading edges are being considered for use on hypersonic vehicles to limit maximum temperatures to values below material reuse limits and to eliminate the need to actively cool the leading edges. The development of a refractory-composite/heat-pipe-cooled leading edge has evolved from the design stage to the fabrication and testing of heat pipes embedded in carbon/carbon (C/C). A three-foot-long, molybdenum-rhenium heat pipe with a lithium working fluid was fabricated and tested at an operating temperature of 2460°F to verify the individual heat-pipe design. Following the fabrication of this heat pipe, three additional heat pipes were fabricated and embedded in C/C. The C/C heat-pipe test article was successfully tested using quartz lamps in a vacuum chamber in both a horizontal and vertical orientation. Start up and steady state data are presented for the C/C heat-pipe test article. Radiography and eddy current evaluations were performed on the test article.

14. SUBJECT TERMS
Heat pipes, liquid metals, carbon/carbon, leading edges

15. NUMBER OF PAGES
34

16. PRICE CODE
A03

17. SECURITY CLASSIFICATION OF REPORT	18. SECURITY CLASSIFICATION OF THIS PAGE	19. SECURITY CLASSIFICATION OF ABSTRACT	20. LIMITATION OF ABSTRACT
Unclassified	Unclassified	Unclassified	